Biogeosciences Discuss., https://doi.org/10.5194/bg-2017-510
Manuscript under review for journal Biogeosciences
Discussion started: 4 December 2017

Biogeosciences Discussions Open Access EGU

Effects of elevated CO_2 and temperature on phytoplankton community biomass, species composition and photosynthesis during an autumn bloom in the Western English Channel

Matthew Keys[1, 2], Gavin Tilstone[1*], Helen S. Findlay[1], Claire E. Widdicombe[1] and Tracy Lawson[2].

[1] Plymouth Marine Laboratory, Prospect Place, The Hoe, Plymouth, PL1 3DH, UK.

[2] University of Essex, Wivenhoe Park, Colchester, CO4 3SQ, UK.

Correspondence to: G. Tilstone (ghti@pml.ac.uk)

Abstract

The combined effects of elevated pCO_2 and temperature were investigated during an autumn phytoplankton bloom in the Western English Channel (WEC). A full factorial 36-day microcosm experiment was conducted under year 2100 predicted temperature (+ 4.5 °C) and pCO_2 levels (800 µatm). The starting phytoplankton community biomass was 110.2 (± 5.7 sd) mg carbon (C) m^{-3} and was dominated by dinoflagellates (~50 %) with smaller contributions from nanophytoplankton (~13 %), cryptophytes (~11 %)and diatoms (~9 %). Over the experimental period total biomass was significantly increased by elevated pCO_2 (20-fold increase) and elevated temperature (15-fold increase). In contrast, the combined influence of these two factors had little effect on biomass relative to the ambient control. The phytoplankton community structure shifted from dinoflagellates to nanophytoplankton at the end of the experiment in all treatments. Under elevated pCO_2 nanophytoplankton contributed 90% of community biomass and was dominated by *Phaeocystis* spp., while under elevated temperature nanophytoplankton contributed 85% of the community biomass and was dominated by smaller nano-flagellates. Under ambient conditions larger nano-flagellates dominated while the smallest nanophytoplankton contribution was observed under combined elevated pCO_2 and temperature (~40 %). Dinoflagellate biomass declined significantly under the individual influences of elevated pCO_2, temperature and ambient conditions. Under the combined effects of elevated pCO_2 and temperature, dinoflagellate biomass almost doubled from the starting biomass and there was a 30-fold increase in the harmful algal bloom (HAB) species, *Prorocentrum cordatum*. Chlorophyll a normalised maximum photosynthetic rates (P^B_m) increased > 6-fold under elevated pCO_2 and > 3-fold under elevated temperature while no effect on P^B_m was observed when pCO_2 and temperature were elevated simultaneously. The results suggest that future increases in temperature and pCO_2 do not appear to influence coastal phytoplankton

Biogeosciences Discuss., https://doi.org/10.5194/bg-2017-510
Manuscript under review for journal Biogeosciences
Discussion started: 4 December 2017

productivity during autumn in the WEC which would have a negative feedback on atmospheric CO_2.

1. Introduction

Oceanic uptake of atmospheric CO_2 has increased by ~42% over pre-industrial levels, with an on-going annual increase of ~0.4%. Current CO_2 level has reached ~400 µatm and has been predicted to rise to >700 µatm by the end of this century (Alley *et al.*, 2007), with estimates exceeding 1000 µatm (Raupach *et al.*, 2007; Raven *et al.*, 2005). The oceans are absorbing CO_2 from the atmosphere, which results in a shift in oceanic carbonate chemistry resulting in a decrease in seawater pH or 'Ocean Acidification' (OA). The projected increase in atmospheric CO_2 and corresponding increase in ocean uptake, is predicted to result in a decrease in global mean seawater pH of 0.3 units below the present value of 8.1 to 7.8 (Wolf-gladrow et al., 1999). Under this scenario, the shift in dissolved inorganic carbon (DIC) equilibria has wide ranging implications for phytoplankton photosynthetic carbon fixation rates and growth (Riebesell, 2004).

Concurrent with OA, elevated atmospheric CO_2 and other climate active gases have warmed the planet by ~0.6 °C over the past 100 years (IPCC, 2007). Atmospheric temperature has been predicted to rise by a further 1.8 to 4 °C by the end of this century (Alley et al., 2007). Phytoplankton metabolic activity may be accelerated by increased temperature (Eppley, 1972), which can vary depending on the phytoplankton species and their physiological requirements (Beardall and Stojkovic, 2006). Long-term data sets already suggest that ongoing changes in coastal phytoplankton communities are likely due to climate shifts and other anthropogenic influences (Edwards et al., 2006; Smetacek and Cloern, 2008; Widdicombe et al., 2010). The response to OA and temperature can potentially alter the community composition, community biomass and photo-physiology. Understanding how these two factors may interact (synergistically or antagonistically) is critical to our understanding and for predicting future primary productivity (Boyd and Doney, 2002).

Laboratory studies of phytoplankton species in culture and studies on natural populations in the field have shown that most species exhibit sensitivity, in terms of growth and photosynthetic rates, to elevated pCO_2 and temperature individually. To date, only a few studies have investigated the interactive effects of these two stressors on natural populations (e.g. Coello-Camba et al., 2014; Feng et al., 2009; Gao et al., 2017; Hare et al., 2007). Most laboratory studies have varied results with species-specific responses, for example, with the diatom *Thalassiosira weissflogii,* pCO_2 elevated to 1000 µatm and + 5 °C temperature increase synergistically enhanced growth, while the same conditions resulted in a reduction in growth

for the diatom *Dactyliosolen fragilissimus* (Taucher et al., 2015). Although there have been fewer studies on dinoflagellates, similar variability in responses has been observed, e.g. (Errera et al., 2014; Fu et al., 2008). In natural populations, elevated pCO_2 has stimulated growth in pico- and nanophytoplankton communities (Engel et al., 2008) while increased temperature has reduced biomass of these groups (Moustaka-Gouni et al., 2016). In a recent field study on natural phytoplankton communities, elevated temperature (+ 3°C above ambient) enhanced community biomass in natural populations but the combined influence of elevated temperature and pCO_2 caused a reduction in biomass (Gao et al., 2017).

Phytoplankton species composition, abundance and biomass has been measured at the time-series station L4 in the western English Channel (WEC) since 1992, to evaluate how global changes could drive future shifts in phytoplankton community structure and carbon biogeochemistry. To compliment the biological time series, key environmental parameters for monitoring the health and state of the WEC are measured weekly including depth profiles of seawater temperature. Dissolved inorganic carbon (DIC) and total alkalinity (TA) has been sampled at station L4 since 2008. Over the past 50 years a 0.5 °C warming has been observed in the WEC (Smyth et al., 2010). The DIC and TA time series is relatively short and as such there is no significant trend in the calculated pCO_2, although it has shown an increase.

Based on the existing literature, the working hypotheses of this study are that: (1) community biomass will increase differentially under individual treatments of elevated temperature and pCO_2; (2) elevated pCO_2 will lead to taxonomic shifts due to differences in species-specific CO_2 concentrating mechanisms and/or RuBisCO specificity; (3) photosynthetic carbon fixation rates will increase differentially under individual treatments of elevated temperature and pCO_2; (4) elevated temperature will lead to taxonomic shifts due to species-specific thermal optima; (5) temperature and pCO_2 elevated simultaneously will have synergistic effects.

The objectives of the study were to investigate: 1) the combined effects of elevated pCO_2 and temperature on phytoplankton community structure, biomass and photosynthetic carbon fixation rates during the autumn transition from diatoms and dinoflagellates to nanophytoplankton at station L4; 2) assess the natural variability in phytoplankton community structure and the carbon biomass of the dominant species observed in the experimental community relative to long-term observations at station L4 over two decades (1993-2014); and 3) assess the distribution of biomass of the dominant species observed at the end of the experiment relative to the in-situ gradients of temperature and pCO_2 observed at station L4. The effects of elevated pCO_2 and temperature on phytoplankton succession in autumn is presently unknown.

Biogeosciences Discuss., https://doi.org/10.5194/bg-2017-510
Manuscript under review for journal Biogeosciences
Discussion started: 4 December 2017

2. Materials and methods

2.1 Time series, phytoplankton community composition

Station L4 (50° 15'N, 4° 13'W) is located 13 km SSW of Plymouth in a water depth of ~54 m (Harris, 2010) and is regarded as one of Europe's principal coastal time series sites. Sampling is conducted on a weekly basis (weather permitting) and has been on-going since 1992 (http://www.westernchannelobservatory.org). Phytoplankton taxonomic composition was enumerated from seawater samples collected from 10 m depth, fixed with 2 % (final concentration) acid Lugol's iodine solution and analysed by inverted light microscopy using the Utermöhl counting technique (Utermöhl, 1958; Widdicombe *et al.*, 2010). For phytoplankton carbon biomass values; taxa-specific mean cell bio-volumes were calculated following Kovala & Larrance, (1966) and converted to carbon using the equations of Menden-Deuer & Lessard, (2000).

2.2 Perturbation experiment, sampling and experimental set-up

Experimental seawater containing a natural phytoplankton community was sampled at station L4 on 7th October 2015 from 10 m depth (40 L). The experimental seawater was gently pre-filtered through a 200 µm Nitex mesh to remove zooplankton grazers, into two 20 L acid-cleaned carboys. In addition, 320 L of seawater was collected into sixteen 20 L acid-cleaned carboys from the same depth for use as experimental media. Immediately upon return to the laboratory the media seawater was filtered through an in-line 0.2 and 0.1 µm filter (Acropak™, Pall Life Sciences) then stored in the dark at 14 °C until use. The experimental seawater was gently and thoroughly mixed and transferred in equal parts from each carboy (to ensure homogeneity) to sixteen 2.5 L borosilicate incubation bottles (4 sets of 4 replicates). The remaining experimental seawater was sampled for initial (T0) concentrations of nutrients, chlorophyll *a*, total alkalinity, dissolved inorganic carbon, particulate organic carbon (POC) and nitrogen (PON) and was also used to characterise the starting experimental phytoplankton community. The incubation bottles were placed in an outdoor simulated in-situ incubation culture system and each set of replicates were linked to one of four 22 L reservoirs filled with the filtered seawater media. Neutral density spectrally corrected blue filters (Lee Filter no. 301) were placed between polycarbonate sheets and mounted to the top, sides and ends of the incubation system to provide ~50 % irradiance, approximating PAR measured at 10 m depth at station L4 on the day of sampling prior to starting experimental incubations. The media was aerated with CO_2 free air and 5 % CO_2 in air precisely mixed using a mass flow controller (Bronkhorst UK Limited) and used for the microcosm dilutions as per the following experimental design: (1) control (390 µatm pCO_2, 14.5 °C matching station L4 in-situ values),

(2) high temperature (390 µatm pCO_2, 18.5 °C), (3) high pCO_2 (800 µatm pCO_2, 14.5 °C) and (4) combination (800 µatm pCO_2, 18.5 °C).

Initial nutrient concentrations (measured at 0.24 µM nitrate + nitrite, 0.086 µM phosphate and 2.14 µM silicate on 7th October 2015) were amended to 8 µM nitrate+nitrite and 0.5 µM phosphate to provide favourable growth conditions. As the phytoplankton community was sampled over the transitional phase from diatoms and dinoflagellates to nanophytoplankton, the in-situ silicate concentration was maintained to reproduce the silicate concentrations typical of this time of year (Smyth et al., 2010). Media transfer and sample acquisition was facilitated by peristaltic pumps and semi-continuous daily dilution rates were set between 10-13 % of the incubation bottle volume following 48 hrs acclimation in batch culture. CO_2 enriched seawater was added to the high CO_2 treatment replicates every 24 hrs, acclimating the natural phytoplankton population to increments of elevated pCO_2 from ambient to ~800 µatm over 8 days followed by maintenance at ~800 µatm as per the method described by Schulz *et al*, (2009). This protocol was preferred since some phytoplankton species are inhibited by the mechanical effects of direct bubbling (Riebesell et al., 2010; Shi et al., 2009) which can cause a reduction in growth rates and the formation of aggregates (Love et al., 2016). pH was monitored daily to adjust the pCO_2 of the experimental media (+/-) prior to dilutions to maintain target pCO_2 levels in the incubation bottles.

2.3 Analytical methods, experimental seawater

2.3.1 Chlorophyll *a*

Chlorophyll *a* (Chl a) was measured in each incubation bottle. 100 mL triplicate samples from each replicate were filtered onto 25 mm GF/F filters (nominal pore size 0.7 µm), extracted in 90 % acetone overnight at -20 °C and chl *a* was estimated on a Turner Trilogy ™ fluorometer using the non-acidified method of Welschmeyer (1994). The fluorometer was calibrated against a stock Chl *a* standard (*Anacystis nidulans*, Sigma Aldrich, UK), the concentration of which was determined with a Perkin Elmer™ spectrophotometer at wavelengths 663.89 and 750.11 nm. Samples for Chl *a* were taken every 2-3 days.

2.3.2 Carbonate system

70 mL samples for total alkalinity (TA) and dissolved inorganic carbon (DIC) analysis were collected from each experimental replicate, stored in amber borosilicate bottles with no head space and fixed with 40 µL of super-saturated Hg_2Cl_2 solution for later determination (Apollo SciTech™ Alkalinity Titrator AS-ALK2; Apollo SciTech™ AS-C3 DIC analyser, with analytical precision of 3 µmol kg^{-1}). Duplicate measurements were made for TA and triplicate

measurements for DIC. Carbonate system parameter values for media and treatment samples were calculated from TA and DIC measurements using the programme CO_2sys (Pierrot et al., 2006) with dissociation constants of carbonic acid of Mehrbach *et al*., (1973) refitted by Dickson and Millero (Dickson and Millero, 1987). Samples for TA and DIC were taken every 2-3 days.

2.3.3 Phytoplankton community analysis

Phytoplankton community analysis was performed by flow cytometry (Becton Dickinson Accuri ™ C6) for the 0.2 to 18 µm size fraction following Tarran *et al.*, (2006) and inverted light microscopy was used to enumerate cells > 18 µm (BS EN 15204,2006). For flow cytometry, 2 mL samples fixed with glutaraldehyde to a final concentration of 2 % were flash frozen in liquid nitrogen and stored at -80 °C for later analysis. For inverted light microscopy, 140 mL samples were fixed with 2 % (final concentration) acid Lugol's iodine solution and analysed by inverted light microscopy (Olympus™ IMT-2) using the Utermöhl counting technique (Utermöhl, 1958; Widdicombe *et al.*, 2010). Phytoplankton community samples were taken at T0, T10, T17, T24 and T36.

2.3.4 Phytoplankton community biomass

The smaller size fraction identified and enumerated through flow cytometry; picophytoplankton, nanophytoplankton, *Synechoccocus*, coccolithophores and cryptophytes were converted to carbon biomass (mg C m^{-3}) using a spherical model to calculate mean cell volume:

$$(\frac{4}{3} * \pi * r^3)$$

and a conversion factor of 0.22 pg C μm^{-3} (Booth, 1988). A conversion factor of 0.285 pg C μm^{-3} was used for coccolithophores (Tarran et al., 2006) and cell a volume of 113 μm^3 and carbon $cell^{-1}$ value of 18 pg applied for *Phaeocystis* spp. (Widdicombe *et al.*, 2010). *Phaeocystis* spp. were identified and enumerated by flow cytometry separately to the nanophytoplankton class due to high observed abundance in in the high pCO_2 treatment. Mean cell measurements of individual species/taxa were used to calculate cell bio-volume for the 18 µm + size fraction according to Kovala and Larrance (1966) and converted to biomass according to the equations of Menden-Deuer & Lessard, (2000).

2.3.5 POC and PON

Samples for particulate organic carbon (POC) and particulate organic nitrogen (PON) were taken at T0, T15 and T36.150 mL samples were taken from each replicate and filtered under gentle vacum onto pre-ashed 25mm glass fibre filters (GF/F, nominal pore size 0.7 µm). Filters

were stored in acid washed petri-slides at -20 °C until further processing. Sample analysis was conducted using a Thermoquest Elemental Analyser (Flash 1112). Acetanilide standards (Sigma Aldrich, UK) were used to calibrate measurements of carbon and nitrogen and also used during the analysis to account for any drift in measured values.

2.3.6 Chl fluorescence-based photophysiology

Photosystem II (PSII) variable Chl fluorescence parameters were measured using a fast repetition rate fluorometer (FRRf) (FastOcean sensor in combination with an Act2Run laboratory system, Chelsea Technologies, West Molesey, UK). The excitation wavelengths of the FRRf's light emitting diodes (LEDs) were 450, 530 and 624 nm. The instrument was used in single turnover mode with a saturation phase comprising 100 flashlets on a 2 µs pitch and a relaxation phase comprising 40 flashlets on a 50 µs pitch. Measurements were conducted in a temperature controlled chamber at 15 °C. The minimum (F_o) and maximum (F_m) Chl fluorescences were estimated according to Kolber et al., (1998). Maximum quantum yields of PSII were calculated as:

$$F_v / F_m = (F_m - F_o) / F_m$$

PSII electron flux was calculated on a volume basis (JV_{PSII}; mol e^- m^{-3} d^{-1}) using the absorption algorithm (Oxborough et al., 2012) following spectral correction by normalising the FRRf LED emission to the white spectra using Fast^{PRO} 8 software. This step required inputting the experimental phytoplankton community fluorescence excitation spectra values (FES). Since we did not measure the FES of our experimental samples, we used mean literature values for each phytoplankton group calculated proportionally (based on percentage contribution to total estimated biomass per phytoplankton group) as representative values for our experimental samples. The JV_{PSII} rates were converted to Chl specific carbon fixation rates (mg C (mg Chl *a*)$^{-1}$ m^{-3} h^{-1}), calculated as:

$$JV_{PSII} \times \varphi_{E:C} \times MW_C / \text{Chl } a$$

where $\varphi_{E:C}$ is the electron requirement for carbon uptake (molecule CO_2 (mol electrons)$^{-1}$), MW_C is the molecular weight of carbon and Chl a is the Chl *a* measurement specific to each sample. Chl specific JV_{PSII} based photosynthesis-irradiance curves were conducted in replicate batches between 10:00 – 16:00 to account for variability over the photo-period at between 8 - 14 irradiance intensities. The maximum intensity applied was adjusted according to ambient natural irradiance on the day of sampling. Maximum photosynthetic rates of carbon fixation (P^B_m), the light limited slope (α^B) and the light saturation point of photosynthesis (I_k) were estimated by fitting the data to the model by Webb et al., (1974):

$P^B = (1\text{-}e \times (-\alpha \times I/P^B{}_m))$

Samples for FRRf fluorescence-based light curves were taken at T36.

2.4 Statistical analysis

To test for effects of high pCO_2, high temperature and high pCO_2 x high temperature on the measured response variables (Chl *a*, total community biomass, POC, PON, photosynthetic parameters and biomass of individual species), generalised least squares models with the factors pCO_2, temperature and time (and all interactions) were applied to the data between T0 and T36 incorporating an auto-regressive correlation structure of the order (1) to account for auto correlation. To test for significant differences between experimental treatments at T36 in all measured parameters, generalized linear models were applied to the data. Where main effects were established, pairwise comparisons were performed using the method of Herberich *et al.*, (2010) for data with non-normality and/or heteroscedasticity. Weekly biomass values from the L4 time-series were averaged over years to elucidate the variability and seasonal cycles of the dominant species observed in the experimental community at T36, relative to the time-series observations. The distribution of these species biomass at station L4 was also analysed relative to the in-situ gradients of temperature (1993-2014) and pCO_2 (2008-2014) using frequency histograms. Analyses were conducted using the R statistical package (R Core Team (2014). R: A language and environment for statistical computing. R Foundation for Statistical Computing, Vienna, Austria).

3. Results

Chl *a* concentration in the WEC ranged between 0.02-~5 mg m^{-3} from 30 September - 6th October 2015, with a concentration of ~1.6 mg m^{-3} at station L4 (**Fig. 1 A**). Over the period leading up to phytoplankton community sampling, increasing nitrate and silicate concentrations coincided with a Chl *a* peak on 23rd September (**Fig. 1 B**). Routine net trawl (20 µm) sample observations indicated a phytoplankton community dominated by the diatoms *Leptocylindrus danicus* and *L. minimus* with a lower presence of the dinoflagellates *Prorocentrum cordatum*, *Heterocapsa* spp. and *Oxytoxum gracile*. Following decreasing nitrate concentrations, this community transitioned to a *P. cordatum* bloom on 29th September, the week before experimental community sampling (data not shown).

3.1 Experimental carbonate system

Equilibration to the target high pCO_2 values (800 µatm) within the high pCO_2 and combination treatments was achieved at T10 (**Fig. 2 A**). These treatments were slowly acclimated to increasing levels of pCO_2 over 7 days (from the initial dilution at T3) while the control and high

temperature treatments were acclimated at the same ambient carbonate system values as that from station L4 on the day of sampling. Following equilibration, the mean pCO_2 values within the control and high temperature treatments were 394.9 (± 4.3 sd) and 393.2 (± 4.8 sd) µatm respectively, while in the high pCO_2 and combination treatments mean pCO_2 values were 822.6 (± 9.4) and 836.5 (± 15.6 sd) µatm, respectively. Carbonate system values remained stable throughout the experiment (**Fig. 2 B-D**).

3.2 Experimental temperature treatments

Mean temperatures in the control and high pCO_2 treatments were 14.1 (± 0.35 sd) °C and in the high temperature and combination treatments the mean temperatures were 18.6 (± 0.42 sd) °C. There was a mean temperature difference between the ambient and high temperature treatments of 4.46 (± 0.42 sd) °C (Supporting information, Fig. S1 A & B).

3.3 Chlorophyll *a*

Mean Chl *a* in the experimental seawater at T0 was 1.64 (± 0.02 sd) mg m^{-3} (**Fig. 3 A**). This decreased in all treatments between T0 to T7, to ~0.1 (± 0.09, 0.035 and 0.035 sd) mg m^{-3} in the control, high pCO_2 and combination treatments, while in the high temperature treatment at T7 Chl *a* was 0.46 mg m^{-3} (± 0.29 sd). From T7 to T12 there was an increase in Chl *a* in all treatments which was highest in the combination (4.99 mg m^{-3} ± 0.69 sd) and high pCO_2 treatments (3.83 mg m^{-3} ± 0.43 sd) (**Table 1**). At T36 Chl *a* concentration in the combination treatment was significantly higher than all other treatments at 6.87 (± 0.58 sd) mg m^{-3} (**Table 2**) while the high temperature treatment concentration was significantly higher than the control and high pCO_2 treatments at 4.77 (± 0.44 sd) mg m^{-3} (**Table 2**). Mean concentrations for the control and high pCO_2 treatments at T36 were not significantly different at 3.30 (± 0.22 sd) and 3.46 (± 0.35 sd) mg m^{-3} respectively (pairwise comparison $t = 0.78$, $p = 0.858$).

3.4 Phytoplankton biomass

The starting biomass in all treatments was 110.2 (± 5.7 sd) mg C m^{-3} (**Fig. 3 B**) and the community biomass was dominated by dinoflagellates (~50%) with smaller contributions from nanophytoplankton (~13%), cryptophytes (~11%), diatoms (~9%), coccolithophores (~8%), *Synechococcus* (~6%) and picophytoplankton (~3%). Total biomass increased significantly in all treatments over time (**Table 1**) and at T10, it was significantly higher in the high temperature treatment when the biomass reached 752 (± 106 sd) mg C m^{-3}. At T36 however, total biomass was significantly higher in the high pCO_2 treatment (**Table 1**) and reached 2481

(± 182.68 sd) mg C m^{-3}, which increased more than 20-fold from T0. Total biomass in the high temperature treatment increased more than 15-fold to 1735 (± 169.24 sd) mg C m^{-3} at T36 and was significantly higher than the combination treatment and ambient control, which were 525 (± 28.02 sd) mg C m^{-3} and 378 (± 33.95 sd) mg C m^{-3}, respectively (**Table 2**).

Measured POC followed the same trends as estimated biomass in all treatments between T0 and T36 (**Fig. 3 C**) and despite some variability between the two measures, POC was within the range of estimates (R^2 = 0.914, **Fig. 3 D**). At T36, POC was significantly greater in the high pCO_2 treatment (2086 ± 155.19 sd mg m^{-3}) followed by the high temperature treatment (1594 ± 162.24 sd mg m^{-3}), which were significantly greater than the control and combination treatment (**Table 1**). PON followed the same trends as POC over the course of the experiment (**Fig. 3 E, Table 1**): at T36 concentrations were 147 (± 12.99 sd) and 133 (± 15.59 sd) mg m^{-3} in the high pCO_2 and high temperature treatments respectively, while PON was 57.75 (± 13.07 sd) mg m^{-3} in the combination treatment and 47.18 (± 9.32 sd) mg m^{-3} in the control (**Table 1**). POC:PON ratios increased significantly over time in all treatments except for the control. The largest increase of 33 %, from 10.72 to 14.26 mg m^{-3} (± 1.73 sd) was in the high pCO_2 treatment, followed by an increase of 32 % to 9.83 (± 1.82 sd) mg m^{-3} in the combination treatment, and an increase of 17 % to 12.09 (± 2.14 sd) mg m^{-3} in the high temperature treatment. In contrast, the POC:PON ratio in the control declined by 20 % from T0 to T36, from 10.33 to 8.26 (± 0.50 sd) mg m^{-3} (**Fig. 3 F, Table 1**).

3.5 Community composition

At T36 diatoms dominated the phytoplankton community biomass in the ambient control with a substantial contribution from nanophytoplankton (**Fig. 4 A**), while the high temperature and high pCO_2 treatments exhibited near mono-specific dominance of nanophytoplankton (**Figs. 4 B & C**). The most diverse community was in the combination treatment where dinoflagellates and *Synechococcus* became more prominent (**Fig. 4 D**).

Between T10 and T24 the community shifted to nanophytoplankton in all experimental treatments. This dominance was maintained through to T36 in the high temperature and high pCO_2 treatments whereas in the ambient control and combination treatment, the community shifted away from nanophytoplankton (**Fig. 5 A**). At T36 nanophytoplankton biomass was significantly higher in the high pCO_2 treatment followed by the high temperature treatment (**Table 2**) when biomass attained 2216 (± 189.67 sd) mg C m^{-3} and 1489 (± 170.32 sd) mg C m^{-3}, respectively. In the combination treatment nanophytoplankton biomass was 238 (± 14.16 sd) mg C m^{-3} at T36 which was significantly higher compared to the ambient control (162 ± 20.02 sd mg C m^{-3}; **Table 2**). In addition to significant differences in nanophytoplankton biomass

amongst the experimental treatments, treatment-specific differences in cell size was observed. Larger nano-flagellates dominated the control (mean cell diameter of 6.34 µm), smaller nano-flagellates dominated the high temperature and combination treatments (mean cell diameters of 3.61 µm and 4.28 µm) whereas *Phaeocystis* spp. dominated the high pCO_2 treatment (mean cell diameter 5.04 µm) and was not observed in any other treatment (Supporting Information, Fig. S2 A-D).

Low starting biomass of diatoms at T0 was dominated by *Coscinodiscus wailessi* (48 %; 4.99 mg C m^{-3}), *Pleurosigma* (25 %; 2.56 mg C m^{-3}) and *Thalassiosira subtilis* (19 %; 1.94 mg C m^{-3}). Small biomass contributions were made by *Navicula distans*, undetermined pennate diatoms and *Cylindrotheca closterium*. Biomass in the diatom group remained low from T0 to T24 but increased at T36 in all treatments, with significantly higher biomass in the high pCO_2 treatment (235 ± 21.41 sd mg C m^{-3}, **Fig. 5 B, Table 2**). The highest diatom contribution to total community biomass at T36 was in the ambient control (52 % of biomass; 198 ± 17.28 sd mg C m^{-3}). In both the high temperature and combination treatments diatom biomass was significantly lower at T36 (151 ± 10.94 sd and 124 ± 19.16 sd mg C m^{-3}, respectively). In all treatments at T36, diatom biomass shifted away from dominance of the larger *C. Wailessii* to the comparatively smaller *C. closterium*, *N. distans*, *T. subtilis* and *Tropidoneis* spp., the relative contributions of which were treatment-specific. Overall *N. distans* dominated diatom biomass in all treatments at T36 (ambient control: 112 ± 24.86 sd mg C m^{-3}, 56 % of biomass; high temperature: 106 ± 17.75 sd mg C m^{-3}, 70 % of biomass; high pCO_2: 152 ± 19.09 sd mg C m^{-3}, 61 % of biomass; and combination: 111 ± 20.97 sd mg C m^{-3}, 89 % of biomass; Supporting Information, Fig. S3 A-D).

The starting dinoflagellate community was dominated by *Gyrodinium spirale* (91 %; 49 mg C m^{-3}), with smaller contributions from *Katodinium glaucum* (5 %; 2.76mg C m^{-3}), *Prorocentrum cordatum* (3 %; 1.78 mg C m^{-3}) and undetermined *Gymnodiniales* (1 %; 0.49 mg C m-3). At T36 dinoflagellate biomass was significantly higher in the combination treatment (90 ± 16.98 sd mg C m^{-3}, **Fig. 5 C, Table 2**) followed by the high temperature treatment (57 ± 6.87 sd mg C m^{-3}, **Table 2**). There was no significant difference in dinoflagellate biomass between the high pCO_2 treatment and ambient control at T36 when biomass was low. In the combination treatment, dinoflagellate biomass shifted away from the larger *G. spirale* and was dominated by *P. cordatum* which contributed 59 ± 12.95 sd mg C m^{-3} (66 % of biomass in this group).

Synechococcus biomass was significantly higher at T36 in the combination treatment (59.9 ± 4.30 sd mg C m^{-3}, **Fig. 5 D, Table 2**) followed by the high temperature treatment (30 ± 5.98 sd mg C m^{-3}, **Table 2**). In both the high pCO_2 treatment and ambient control at T36 *Synechococcus* biomass was low (~7 mg C m^{-3} in both treatments). Relative to the other phytoplankton groups,

biomass of picophytoplankton (**Fig. 5 E**), cryptophytes (**Fig. 5 F**) and coccolithophores (**Fig. 5 G**) remained low in all treatments throughout the experiment. Though picophytoplankton responded positively to the high pCO_2 and combination treatments at T36 (high pCO_2: 6.93 ± 0.63 sd mg C m^{-3}; combination: 11.26 ± 0.79 sd mg C m^{-3}; **Table 2**).

3.6 Chl fluorescence-based photophysiology

At T36, FRRf PI parameters were strongly influenced by the experimental treatments. P^B_m was significantly higher in the high pCO_2 treatment (18.93 mg C (mg Chl *a*)$^{-1}$ m^{-3} h^{-1}), followed by the high temperature treatment (9.58 mg C (mg Chl *a*)$^{-1}$ m^{-3} h^{-1}; **Fig. 6, Tables 3 & 4**). There was no significant difference in P^B_m between the ambient control and combination treatment (2.77 and 3.02 mg C (mg Chl *a*)$^{-1}$ m^{-3} h^{-1}). Light limited photosynthetic efficiency (α^B) also followed the same trend and was significantly higher in the high pCO_2 treatment (0.13 mg C (mg Chl *a*)$^{-1}$ m^{-3} h^{-1} (µmol photon m^{-2} s^{-1})$^{-1}$) followed by the high temperature treatment (0.09 mg C (mg Chl *a*)$^{-1}$ m^{-3} h^{-1} (µmol photon m^{-2} s^{-1})$^{-1}$) (**Tables 3 & 4**). α^B was low in both control and combination treatments (0.03 and 0.04 mg C (mg Chl *a*)$^{-1}$ m^{-3} h^{-1} (µmol photon m^{-2} s^{-1})$^{-1}$, respectively). The light saturation point of photosynthesis (I_k) was significantly higher in the high pCO_2 treatment relative to all treatments where I_k was 144.13 µmol photon m^{-2} s^{-1}, though significantly lower in the combination treatment relative to both the high pCO_2 and high temperature treatments (**Tables 3 & 4**).

3.7 Natural variability of biomass in the WEC, station L4 time series.

Nanophytoplankton is a critical component of the station L4 carbon budget. The mean annual total nanophytoplankton biomass over the time series (1993-2014) was 586 (± 16.54 sd) mg C m^{-3} with maximum annual biomass of 1182 mg C m^{-3} in 2002 (62 % of total annual phytoplankton biomass) and minimum annual biomass of 262 mg C m^{-3} in 2008 (23 % of total annual phytoplankton biomass). In 8 of the 21 years of time series observations, nanophytoplankton contributed more than 40 % of the station L4 carbon budget. Consistently over the seasonal cycle at L4, mean nanophytoplankton biomass > 10 mg C m^{-3} occurred from early April until the end of October, exhibiting sustained long-term seasonality relative to other phytoplankton groups, though maximal biomass was constrained between April and the 3rd week of June with one exception (**Fig. 7 A**).

N. distans dominated diatom biomass in the experimental communities though was found to be a very minor component of the diatom carbon budget at station L4 (0.04 % of total annual diatom biomass). Weekly *N. distans* biomass averaged over the time series was very low and ranged from below the limit of detection to ~0.2 mg C m^{-3} with maximum total annual biomass

of ~0.5 mg C m^{-3} in 2005 (**Fig. 7 B**). Seasonality of maximal *N. distans* biomass was constrained to September-October when the mean maximal biomass was 0.03 mg C m^{-3}.

P. cordatum dominated the dinoflagellate biomass in the experimental communities, and made a significant contribution to total biomass in the combination treatment. Weekly *P. cordatum* biomass averaged over the time series at L4 ranged from 0.004 to 107 mg C m^{-3} and exhibited strong seasonality. Mean total annual *P. cordatum* biomass was 25.5 mg C m^{-3} with maximum annual biomass of 233 mg C m^{-3} in 2006 (minimum annual biomass of 0.004 mg C m^{-3} in 1994). The bloom peak (taken as an increase in biomass > 1.0 mg C m^{-3}) usually occurred in September although as early as mid-June (2001 and 2013) in some cases (**Fig. 7 C**). Mean maximal biomass was 12.7 mg C m^{-3} with positive anomalies occurring in 5 out of 21 years throughout the time-series (ranging from 15 to 107 mg C m^{-3}). *P. cordatum* contributed on average, 9.2 % of the total annual dinoflagellate biomass with a maximum contribution of ~55 % in 2006 and 12 % and 63 % when averaged over the bloom period from mid-June to end-September. *P. cordatum* contributed 3.4 % of total phytoplankton biomass during the bloom period and ~32 % of total phytoplankton biomass in 2006 during an unprecedented bloom when biomass attained 107 mg C m^{-3} in 2006 (**Fig. 7 D**).

Group and species-specific optimal temperature ranges were found when considering how the dominant experimental species were temporally distributed relative to in-situ temperatures: nanophytoplankton exhibited a bi-modal distribution with 31 % biomass between 9-11 °C and 30 % between 15-16.5 °C, with 6 % above 16.5 °C (**Fig. 8 A**). ~60 % of *N. distans* biomass occurred between 14-16 °C and 2 % biomass above 16 °C (**Fig. 8 B**). In contrast, 66 % of *P. cordatum* biomass occurred between 14-16 °C and 24 % above 16 °C (**Fig. 8 C**). Biomass distribution relative to station L4 in-situ pCO_2 levels (2008-2014) also demonstrated group/species-specific optimal ranges. 71 % nanophytoplankton biomass occurred at a pCO_2 range of 245-410 µatm, 24 % 410-515 µatm and 5 % between 515-680 µatm (**Fig. 8 D**). *N. distans* followed a similar trend with 72% biomass between a pCO_2 range of 245-410 µatm, 26% between 410-515 µatm and < 2% beyond 515 µatm (**Fig. 8 E**). By contrast, 97% of *P. cordatum* biomass occurred between 245-410 µatm with 3 % biomass occurring beyond 410 µatm (**Fig. 8 F**).

4. Discussion

Individually, elevated temperature and pCO_2 resulted in the highest biomass and maximum photosynthetic rates (P^B_m), when nanophytoplankton dominated. The interaction of these two factors had little effect on total biomass with values close to the ambient control, and no effect

on P^B_m. The combination treatment, however, exhibited the greatest diversity of phytoplankton functional groups with dinoflagellates and *Synechococcus* becoming more prominent.

Elevated pCO_2 has been shown to enhance the growth and photosynthesis of some phytoplankton species which have active uptake systems for inorganic carbon (Giordano et al., 2005; Reinfelder, 2011). Elevated pCO_2 may therefore lead to lowered energetic costs of carbon assimilation in some species and a redistribution of the cellular energy budget to other processes (Tortell et al., 2002). In the present study, under elevated pCO_2 where the dominant group was nanophytoplankton, the community was dominated by the bloom-forming haptophyte *Phaeocystis* spp. Photosynthetic carbon fixation in *Phaeocystis* spp. is presently near saturation with respect to current levels of pCO_2 (Rost et al., 2003). Inorganic carbon acquisition in this species has been shown to be equal to, or more efficient than that of diatoms. Indeed, in *Phaeocystis* spp, extracellular carbonic anhydrase is regulated by CO_2 (aq), and HCO_3^- is utilized as a carbon source in photosynthesis, indicating more efficient use of CO_2 (Elzenga et al., 2000; Rost et al., 2003), and thus providing an advantage to *Phaeocystis* spp. when more CO_2 is present. Therefore, the increased biomass and photosynthetic carbon fixation seen here under elevated pCO_2 can be attributed to the community shift to *Phaeocystis* spp.. The increased biomass seen in the high temperature treatment in this study, may be attributed to enhanced enzymatic activities, since algal growth commonly increases with temperature until after the optimal range (Boyd et al., 2013; Goldman and Carpenter, 1974; Savage et al., 2004) and optimum growth temperatures for marine phytoplankton are often several degrees higher than environmental temperatures (Eppley, 1972; Thomas et al., 2012).

4.1 Chl *a*

Chl *a* concentration was significantly higher in the combination treatment at T36 when total biomass was lower, but Chl *a* was significantly lower in the high pCO_2 treatment when biomass was significantly higher than all other treatments. This contrasts the results reported in comparable studies as Chl *a* is generally highly correlated with biomass, (e.g. Feng et al., 2009). Similar results were reported however by Hare et al., (2007) which indicates that Chl *a* may not always be a reliable proxy for biomass in mixed communities. Differences in Chl *a* may therefore be attributed to taxonomic differences in community composition.

4.2 Biomass

This study shows that the phytoplankton community response to elevated temperature and pCO_2 is highly variable. pCO_2 elevated to ~800 µatm induced higher community biomass in agreement with Kim et al., (2006) and Riebesell et al., (2007), whereas in other natural community studies no CO_2 effect on biomass was observed (Delille et al., 2005; Maugendre et al.,

2017; Paul et al., 2015). A ~4.5 °C increase in temperature also resulted in higher biomass in this study, similar to the findings of Feng et al., (2009) and Hare et al., (2007) though elevated temperature has previously reduced biomass of natural nanophytoplankton communities in the Western Baltic Sea and Arctic Ocean (Coello-Camba et al., 2014; Moustaka-Gouni et al., 2016). When elevated temperature and pCO_2 were combined, community biomass exhibited little response, similar to the findings of Gao et al., (2017), though an increase in biomass has also been reported (Calbet et al., 2014; Feng et al., 2009). Geographic location and season also play an important role in structuring the community and its response in terms of biomass to elevated temperature and pCO_2, e.g. (Li et al., 2009; Morán et al., 2010).

4.3 Carbon:Nitrogen

In agreement with others, the results of this experiment showed highest increases in C:N under elevated pCO_2 alone (Riebesell et al., 2007). C:N also increased under high temperature, consistent with the findings of Lomas and Glibert, (1999) and Taucher et al., (2015) and was stimulated to a lesser degree when pCO_2 and temperature were elevated simultaneously, which was also observed in the study of Calbet et al., (2014), but contrasts other studies that have observed C:N to be unaffected by the combined influence of elevated pCO_2 and temperature, e.g. (Deppeler and Davidson, 2017; Kim et al., 2006; C. Paul et al., 2015). C:N is a strong indicator of cellular protein content (Woods and Harrison, 2003) and increases under elevated pCO_2 and warming may likely lead to lowered nutritional value of phytoplankton with consequences for zooplankton reproduction and biogeochemical cycles.

4.4 Photosynthetic carbon fixation rates

At T36, under elevated pCO_2 P^B_m was > 6 times higher than the ambient control, which has also been reported in elevated pCO_2 perturbation experiments by Riebesell et al., (2007) and Tortell et al., (2008), but contrasts other observations on natural populations where the effect of elevated pCO_2 alone was found to reduce P^B_m (Feng et al., 2009; Hare et al., 2007). Studies on laboratory cultures have shown that increases in temperature increase photosynthetic rates (Feng et al., 2008; Fu et al., 2007; Hutchins et al., 2007), similar to our findings. We found that there was no effect on P^B_m under the combined treatment which has also been observed in experiments on natural populations (Coello-Camba and Agustí, 2016; Gao et al., 2017). This strongly contrasts the findings of Feng et al., (2009) and Hare et al., (2007) who observed the highest P^B_m when temperature and pCO_2 were elevated simultaneously. Increases in α^B and I_k under elevated pCO_2, and a decrease in these parameters when elevated pCO_2 and temperature were combined is opposite to the trends reported by Feng et al., (2009).

Photosynthetic rates have been demonstrated to decrease beyond a temperature of 20 °C (Raven and Geider, 1988) which can be modified through photoprotective rather than photosynthetic pigments (Kiefer and Mitchell, 1983). This may explain the difference in P^B_m between the high pCO_2 and high temperature treatments (in addition to differences in nanophytoplankton community composition in relation to *Phaeocystis* spp. discussed above), as the experimental high temperature treatment in the present study was ~4.5 ° C higher than ambient.

There was no significant effect of combined elevated pCO_2 and temperature on P^B_m, which was strongly influenced by taxonomic differences between the experimental treatments. Warming has been shown to lead to smaller cell sizes in nanophytoplankton (Atkinson et al., 2003; Peter and Sommer, 2012), which was observed in the combined treatment together with decreased nanophytoplankton biomass. Diatoms also shifted to smaller species with reduced biomass, while dinoflagellate and *Synechococcus* biomass increased at T36. Dinoflagellates are the only photoautotrophs with form II RuBisCO (Morse et al., 1995) which has the lowest carboxylation:oxygenation specificity factor among eukaryotic phytoplankton (Badger et al., 1998), giving dinoflagellates a disadvantage in carbon fixation under present ambient pCO_2 levels. Dinoflagellates generally grow at slower rates in surface waters with high pH (≥9) resulting from photosynthetic removal of CO_2 by previous blooms (Hansen, 2002; Hinga, 2002). Though growth under high pH provides indirect evidence that dinoflagellates possess CCMs, direct evidence is limited and points to the efficiency of CCMs in dinoflagellates as moderate in comparison to diatoms and some haptophytes (Reinfelder, 2011 and references therein). This may explain the lower P^B_m in the combined treatment compared to elevated pCO_2 and temperature individually.

4.5 Community composition

Phytoplankton community structure changes were observed, with a shift from dinoflagellates to nanophytoplankton which was most pronounced under single treatments of elevated temperature and pCO_2. Amongst the nanophytoplankton, a distinct size shift to smaller cells was observed in the high temperature and combination treatments, while in the high pCO_2 treatment *Phaeocystis* spp. dominated. Under combined pCO_2 and temperature at T36 however, dinoflagellate and *Synechococcus* biomass increased at the expense of nanophytoplankton.

An increase in pico- and nanophytoplankton has previously been reported in natural communities under elevated pCO_2 (Bermúdez et al., 2016; Boras et al., 2016; Brussaard et al., 2013; Engel et al., 2008) while no effect on these size classes has been observed in other studies (Calbet et al., 2014; Paulino et al., 2007). Moustaka-Gouni et al., (2016) also found no CO_2 effect

535 on natural nanophytoplankton communities but increased temperature reduced the biomass of
536 this group. Kim et al., (2006) observed a shift from nanophytoplankton to diatoms under
537 elevated pCO_2 alone while a shift from diatoms to nanophytoplankton under combined elevated
538 pCO_2 and temperature has been reported (Hare et al., 2007). A variable response in *Phaeocystis*
539 spp. to elevated pCO_2 has also been reported with increased growth (Chen et al., 2014; Keys et
540 al., 2017), no effect (Thoisen et al., 2015) and decreased growth (Hoogstraten et al., 2012)
541 observed. *Phaeocystis* spp. can outcompete other phytoplankton and form massive blooms (up
542 to 10 g C m^{-3}) with impacts on food webs, global biogeochemical cycles and climate regulation
543 (Schoemann et al., 2005). While not a highly toxic algal species, *Phaeocystis* spp. are considered
544 a harmful algal bloom (HAB) species when biomass reaches sufficient concentrations to cause
545 anoxia through the production of mucus foam which can clog the feeding apparatus of
546 zooplankton and fish (Eilertsen & Raa, 1995).

547 The response of diatoms to elevated pCO_2 and temperature has been variable. For example, A
548 study by Taucher et al., (2015) showed that *Thalassiosira weissflogii* incubated at 1000 µatm
549 pCO_2 increased growth by 8 % while for *Dactyliosolen fragilissimus*, growth increased by 39 %;
550 temperature elevated by + 5°C also had a stimulating effect on *T. weissflogii* but inhibited the
551 growth rate of *D. fragilissimus*; and when the treatments were combined growth was enhanced
552 in *T. weissflogii* but reduced in *D. fragilissimus*. In partial agreement, the results of the present
553 experiment show that elevated pCO_2 increased biomass in diatoms but elevated temperature
554 and the combination of these factors reduced biomass. A distinct size-shift in diatom species
555 was observed in all treatments, from the larger *Coscinodiscus* spp., *Pleurosigma* and
556 *Thalassiosira subtilis* to the smaller *Navicula distans*. This was most pronounced in the
557 combination treatment where *N. distans* contributed 89 % of diatom biomass. *Navicula* spp.
558 previously exhibited a differential response to both elevated temperature and pCO_2. At + 4.5 °C
559 and 960 ppm CO_2 Torstensson et al., (2012) observed no synergistic effects on the benthic
560 *Navicula directa*. Elevated temperature increased growth rates by 43 % while a reduction of 5 %
561 was observed under elevated CO_2. No effects on growth were detected at pH ranging from 8 –
562 7.4 units on *Navicula* spp. (Thoisen et al., 2015), while growth in *N. distans* was significantly
563 stimulated along a CO_2 gradient at a shallow cold-water vent system (Baragi et al., 2015).

564 *Synechococcus* grown under pCO_2 elevated to 750 ppm and temperature elevated by 4 °C
565 resulted in increased growth and a 4-fold increase in P^B_m (Fu et al., 2007) which is similar to the
566 results of the present study.

567 The combination of elevated temperature and pCO_2 significantly increased dinoflagellate
568 biomass which almost doubled, accounting for 17 % of total biomass. This was due to *P.*
569 *cordatum* which increased biomass by more than 30-fold between T0 and T30 (66 % of

570 dinoflagellate biomass in this treatment). Despite the global increase in the frequency of HABs
571 few studies have focussed on the response of dinoflagellates to elevated pCO_2 and temperature.
572 In laboratory studies at 1000 ppm CO_2, growth rates of the HAB species *Karenia brevis* increased
573 by 46 %, at 1000 ppm CO_2 and + 5 °C temperature it's growth increased by 30 % but was
574 reduced under elevated temperature alone (Errera et al., 2014). A combined increase in pCO_2
575 and temperature enhanced both the growth and P^B_m in the dinoflagellate *Heterosigma akashiwo*,
576 whereas in contrast to the present findings, only pCO_2 alone enhanced these parameters in *P.*
577 *cordatum* (Fu et al., 2008).

578 Among HAB species, *P. cordatum* is widely distributed geographically in temperate and
579 subtropical waters, has detrimental effects at the organismal and environmental levels and is
580 potentially harmful to humans via shellfish poisoning (Heil et al., 2005). Recent increases in the
581 frequency, magnitude and distribution of harmful phytoplankton species has focussed attention
582 on the unique physiological, ecological and toxicological aspects of the species involved
583 (Andeson et al., 2002; Hallegraeff, 1993). Ocean acidification combined with warming could
584 potentially affect the growth and toxicity of HAB species (Fu et al., 2012). Recent studies on
585 several diatom and dinoflagellate species suggest that ocean acidification combined with
586 elevated temperature may dramatically increase the toxicity of some harmful groups (e.g.
587 Flores-Moya et al., 2012; Fu et al., 2010; Sun et al., 2011; Tatters et al., 2012). The ecology and
588 bloom dynamics of *P. cordatum* have been well documented in selected environments (e.g.
589 Chesapeake Bay, Baltic Sea). The spread of this species to previously unreported areas through
590 either ballast water transport, aquaculture development, or increasing eutrophication, has been
591 reported (Heil et al., 2005). In Chesapeake Bay *P. cordatum* 'mahogany tides' have been
592 associated with anoxic/hypoxic events, fish kills, aquaculture shellfish kills and the loss of
593 aquatic vegetation (Tango et al., 2005). Over the last two decades *P. cordatum* has established
594 itself as a dominant summer phytoplankton species in the Baltic Sea but so far there are no
595 reports of toxic blooms (Hajdu et al., 2000). However, for the first time a *P. cordatum* bloom was
596 recorded in February 2002 at Bolinao, Northern Philippines and was coincident with a mass
597 aquaculture fish kill resulting in losses estimated at US$120,000 (Azanza et al., 2005). Several
598 clones of *P. cordatum* were found to produce a water-soluble neuro-toxin during bloom decline
599 in culture studies (Grzebyk et al., 1997). More recently, a series of positive bioassays for
600 tetrodotoxins (TTXs) was observed in mussels (Vlamis et al., 2015) which coincided with the
601 simultaneous presence of a *P. cordatum* bloom. Data analysis from previous years (2006 –
602 2012) identified multiple sample cases for toxins in aquaculture production areas coinciding
603 with *P. cordatum* blooms.

In addition to strong links to toxic algal events, mixotrophy has also been reported in *P. cordatum*. In a study by Stoecker et al., (1997) up to 50% of *P. cordatum* sampled from Chesapeake Bay in the summer contained cryptophyte material. The authors concluded that *P. cordatum* feeding is a mechanism for supplementing carbon nutrition and this may explain why the ratio of nanophytoplankton:dinoflagellates was significantly lower in our combination experimental community compared to the other treatments.

4.6 Natural variability of biomass in the WEC, station L4 time series.

During autumn in the WEC, sea surface temperature and pCO_2 start to decline following their respective time series maximal values at station L4. During October, mean seawater temperatures at 10 m decrease from 15.39 °C (± 0.49 sd) to 14.37 °C (± 0.62 sd). Following a period of CO_2 oversaturation in late summer, pCO_2 returns to near-equilibrium at station L4 in October when mean pCO_2 values decrease during this month from 455.32 µatm (± 63.92 sd) to 404.06 µatm (± 38.55 sd) (Kitidis et al., 2012). As is the case with seawater warming, predicted future ocean acidification is likely to impact coastal phytoplankton communities in autumn when the present upper limit of the pCO_2 threshold increases during this period of surface ocean-atmosphere equilibrium (Riebesell, 2004).

From a biological perspective, the autumn period at station L4 is characterised by the decline of the late summer diatom and dinoflagellate blooms (Widdicombe et al., 2010) when biomass of these two groups approaches values close to the time series minima (diatom biomass range: 6.01 (± 6.88 sd) – 2.85 (± 3.28 sd) mg C m^{-3}; dinoflagellate biomass range: 1.75 (± 3.28 sd) – 0.66 (± 1.08 sd) mg C m^{-3}). Typically, over this period nanophytoplankton becomes numerically dominant when biomass of this group ranges from 20.94 (± 33.25 sd) – 9.38 (± 3.31 sd), though the time series shows high variability in this biomass.

Comparative analyses of the WEC time series and the dominant species from the experimental treatments showed that nanophytoplankton contributes significantly to the station L4 carbon budget. The in-situ bimodal distribution of nanophytoplankton biomass at cold and warm temperature ranges indicates a potential tolerance to temperature increase. Most nanophytoplankton biomass occurred at an in-situ pCO_2 range between 245-410 µatm but almost 10 % of biomass was distributed between 515-680 µatm, indicating some tolerance to elevated pCO_2 during periods of CO_2 oversaturation at station L4. The dominant diatom species in the experimental communities, *N. distans*, was a very minor contributor to diatom biomass over the time series with most biomass constrained to very narrow in-situ temperature and pCO_2 ranges of 14-16 ° C and 245-410 µatm. *P. cordatum* dominated dinoflagellate biomass in the combination treatment but was generally a low biomass contributor to dinoflagellate

biomass over the time series, with the exception of one unprecedented bloom in 2006. *P. cordatum* biomass exhibited higher thermal in-situ optima with most biomass observed between 14-16 ° C and almost a quarter of biomass above 16 °C, indicating tolerance to temperature increase, though the majority of biomass at station L4 occurred at times of low in-situ pCO_2 (245-350 µatm) with just 3% beyond 410 µatm. These trends suggest conditions of warming may favour nanophytoplankton and *P. cordatum*, elevated pCO_2 may favour nanophytoplankton and both factors combined may favour both species. These observations are consistent with the experimental results.

5. Implications

Increased biomass, P^B_m and a community shift to nanophytoplankton under individual increases in temperature and pCO_2 suggests a potential positive feedback on atmospheric CO_2, whereby more CO_2 is removed from the ocean, and hence from the atmosphere by photosynthetic activity. The selection of *Phaeocystis* spp. under elevated pCO_2 indicates the potential for negative impacts on ecosystem function and food web structure associated with this species (Schoemann et al., 2005; Verity et al., 2007). However, while more CO_2 is photosynthesised, selection for nanophytoplankton in both of these treatments may actually result in reduced carbon sequestration due to slower sinking rates of these smaller phytoplankton cells (Bopp et al., 2001; Laws et al., 2000). When temperature and pCO_2 were elevated simultaneously, community biomass showed little response and no effects on P^B_m were observed, suggesting a negative feedback on atmospheric CO_2 and climate warming in future warmer high CO_2 oceans. Additionally, combined elevated pCO_2 and temperature significantly modified taxonomic composition, by reducing diatom biomass relative to the ambient control with increasing dinoflagellate biomass dominated by the HAB species, *P. cordatum*. This has implications for fisheries, ecosystem function and human health.

6. Conclusion

These experimental results provide new evidence that increases in pCO_2 coupled with rising sea temperatures may have antagonistic effects on the autumn phytoplankton community in the WEC. Under future global change scenarios, the size range and biomass of diatoms may be reduced with increased dinoflagellate biomass and the selection of HAB species. The experimental simulations of year 2100 temperature and pCO_2 demonstrate that the effects of warming can be offset by elevated pCO_2 potentially reducing coastal phytoplankton productivity and significantly altering the community structure, and in turn these shifts will have consequences on carbon biogeochemical cycling in the WEC.

Data availability: Experimental data used for analysis will be made available (DOI will be created)

Author contributions: Matthew Keys collected, measured, processed and analysed the data and prepared the figures. Drs Gavin Tilstone and Helen Findlay conceived, directed and sought the necessary funds to support the research. Matthew Keys and Dr Gavin Tilstone wrote the paper with input from Claire Widdicombe and Professor Tracy Lawson. Claire Widdicombe supervised and advised on phytoplankton taxonomic classifications.

Competing interests: The authors declare that they have no conflict of interest.

Acknowledgements: G.H.T, H.S.F. and C.E.W were supported by the UK Natural Environment Research Council's (NERC) National Capability – The Western English Channel Observatory (WCO). C.E.W was also partly funded by the NERC and Department for Environment, Food and Rural Affairs, Marine Ecosystems Research Program (Grant no. NE/L003279/1). M.K. was supported by a NERC PhD studentship (grant No. NE/L50189X/1). We thank Glen Tarran for his training, help and assistance with flow cytometry, The National Earth Observation Data Archive and Analysis Service UK (NEODAAS) for their help in providing the MODIS image used in Fig 1. and the crew of RV Plymouth Quest for their helpful assistance during field sampling.

References

Alley, D., Berntsen, T., Bindoff, N. L., Chen, Z. L., Chidthaisong, A., Friedlingstein, P., Gregory, J., G., H., Heimann, M., Hewitson, B., Hoskins, B., Joos, F., Jouzel., Kattsov, V., Lohmann, U., Manning, M., Matsuno, T., Molina, M., Nicholls, N., Overpeck, J., Qin, D.H., Raga, G. Ramaswamy, V., Ren, J.W., Rusticucci, M., Solomon, S. and Somerville, R., Stocker, T.F., Stott, P., Stouffer, R.J. Whetton, P., Wood, R.A. & Wratt, D.: Climate Change 2007. The Physical Science basis: Summary for policymakers. Contribution of Working Group I to the Fourth Assessment Report of the Intergovernmental Panel on Climate Change, in … Climate Change 2007. The Physical Science Basis, Summary for Policy Makers…. [online] Available from: http://scholar.google.com/scholar?hl=en&btnG=Search&q=intitle:Climate+Change+2007+:+The+Physical+Science+Basis+Summary+for+Policymakers+Contribution+of+Working+Group+I+to+the+Fourth+Assessment+Report+of+the#3 (Accessed 24 October 2013), 2007.

Andeson, D., Gilbert, P. and Burkholder, J.: Harmful Algal Blooms and Eutrophication : Nutrient Sources , Composition , and Consequences, Estuaries, 25(4), 704–726, 2002.

Atkinson, D., Ciotti, B. J. and Montagnes, D. J. S.: Protists decrease in size linearly with temperature: ca. 2.5% ° C^{-1}, Proc. R. Soc. B Biol. Sci., 270(1533), 2605–2611,

703 doi:10.1098/rspb.2003.2538, 2003.

704 Azanza, R. V., Fukuyo, Y., Yap, L. G. and Takayama, H.: *Prorocentrum minimum* bloom and its
705 possible link to a massive fish kill in Bolinao, Pangasinan, Northern Philippines, Harmful Algae,
706 4(3), 519–524, doi:10.1016/j.hal.2004.08.006, 2005.

707 Badger, M. R., Andrews, T. J., Whitney, S. M., Ludwig, M., Yellowlees, D. C., Leggat, W. and Price, G.
708 D.: The diversity and coevolution of Rubisco , plastids , pyrenoids , and chloroplast-based CO_2 -
709 concentrating mechanisms in algae 1, Can. J. Bot., (76), 1052–1071, 1998.

710 Baragi, L. V., Khandeparker, L. and Anil, A. C.: Influence of elevated temperature and pCO_2 on the
711 marine periphytic diatom *Navicula distans* and its associated organisms in culture,
712 Hydrobiologia, 762(1), 127–142, doi:10.1007/s10750-015-2343-9, 2015.

713 Beardall, J. and Stojkovic, S.: Microalgae under Global Environmental Change : Implications for
714 Growth and Productivity , Populations and Trophic Flow, Sci. Asia, 1, 1–10,
715 doi:10.2306/scienceasia1513-1874.2006.32(s1).001, 2006.

716 Bermúdez, J. R., Riebesell, U., Larsen, A. and Winder, M.: Ocean acidification reduces transfer of
717 essential biomolecules in a natural plankton community, Sci. Rep., 6(1), 27749,
718 doi:10.1038/srep27749, 2016.

719 Booth, B. C.: Size classes and major taxonomic groups of phytoplankton at two locations in the
720 subarctic pacific ocean in May and August, 1984, Mar. Biol., 97(2), 275–286,
721 doi:10.1007/BF00391313, 1988.

722 Bopp, L. ., Monfray, P. ., Aumont, O. ., Dufresne, J.-L. ., Le Treut, H. ., Madec, G. ., Terray, L. . and
723 Orr, J. C. .: Potential impact of climate change on marine export production, Global Biogeochem.
724 Cycles, 15(1), 81–99, doi:10.1029/1999GB001256, 2001.

725 Boras, J. A., Borrull, E., Cardelu, C., Cros, L., Gomes, A., Sala, M. M., Aparicio, F. L., Balague, V.,
726 Mestre, M., Movilla, J., Sarmento, H., Va, E. and Lo, A.: Contrasting effects of ocean acidification on
727 the microbial food web under different trophic conditions, ICES J. Mar. Sci., 73(73 (3)), 670–679,
728 2016.

729 Boyd, P. W. and Doney, S. C.: Modelling regional responses by marine pelagic ecosystems to
730 global climate change, Geophys. Res. Lett., 29(16), 1–4, 2002.

731 Boyd, P. W., Rynearson, T. A., Armstrong, E. A., Fu, F., Hayashi, K., Hu, Z., Hutchins, D. A., Kudela,
732 R. M., Litchman, E., Mulholland, M. R., Passow, U., Strzepek, R. F., Whittaker, K. A., Yu, E. and
733 Thomas, M. K.: Marine Phytoplankton Temperature versus Growth Responses from Polar to
734 Tropical Waters - Outcome of a Scientific Community-Wide Study, PLoS One, 8(5),

735 doi:10.1371/journal.pone.0063091, 2013.

736 Brussaard, C. P. D., Noordeloos, A. A. M., Witte, H., Collenteur, M. C. J., Schulz, K., Ludwig, A. and
737 Riebesell, U.: Arctic microbial community dynamics influenced by elevated CO_2 levels,
738 Biogeosciences, 10(2), 719–731, doi:10.5194/bg-10-719-2013, 2013.

739 Calbet, A., Sazhin, A. F., Nejstgaard, J. C., Berger, S. a, Tait, Z. S., Olmos, L., Sousoni, D., Isari, S.,
740 Martínez, R. a, Bouquet, J.-M., Thompson, E. M., Båmstedt, U. and Jakobsen, H. H.: Future climate
741 scenarios for a coastal productive planktonic food web resulting in microplankton phenology
742 changes and decreased trophic transfer efficiency., PLoS One, 9(4), e94388,
743 doi:10.1371/journal.pone.0094388, 2014.

744 Chen, S., Beardall, J. and Gao, K.: A red tide alga grown under ocean acidification upregulates its
745 tolerance to lower pH by increasing its photophysiological functions, Biogeosciences, 11, 4829–
746 4837, doi:10.5194/bg-11-4829-2014, 2014.

747 Coello-Camba, A. and Agustí, S.: Acidification counteracts negative effects of warming on diatom
748 silicification, Biogeosciences Discuss., 30(October), 1–19, doi:10.5194/bg-2016-424, 2016.

749 Coello-Camba, A., AgustÃ-, S., Holding, J., Arrieta, J. M. and Duarte, C. M.: Interactive effect of
750 temperature and CO_2 increase in Arctic phytoplankton, Front. Mar. Sci., 1 (October), 1–10,
751 doi:10.3389/fmars.2014.00049, 2014.

752 Delille, B., Harlay, J., Zondervan, I., Jacquet, S., Chou, L., Wollast, R., Bellerby, R. G. J.,
753 Frankignoulle, M., Borges, A. V., Riebesell, U. and Gattuso, J.-P.: Response of primary production
754 and calcification to changes of pCO_2 during experimental blooms of the coccolithophorid
755 *Emiliania huxleyi*, Global Biogeochem. Cycles, 19(2), n/a-n/a, doi:10.1029/2004GB002318,
756 2005.

757 Deppeler, S. L. and Davidson, A. T.: Southern Ocean Phytoplankton in a Changing Climate, Front.
758 Mar. Sci., 4 (February), doi:10.3389/fmars.2017.00040, 2017.

759 Dickson, A. G. and Millero, F. J.: A comparison of the equilibrium constants for the dissociation of
760 carbonic acid in seawater media, Deep Sea Res. Part I Oceanogr. Res. Pap., 34 (111), 1733–1743,
761 1987.

762 Edwards, M., Johns, D., Leterme, S. C., Svendsen, E. and Richardson, A. J.: Regional climate change
763 and harmful algal blooms in the northeast Atlantic, Limnol. Oceanogr., 51(2), 820–829,
764 doi:10.4319/lo.2006.51.2.0820, 2006.

765 Eilertsen, H. and Raa, J.: Toxins in seawater produced by a common phytoplankter : *Phaeocystis*
766 *pouchetii*, J. Mar. Biotechnol., 3(1), 115–119 [online] Available from:

767 http://ci.nii.ac.jp/naid/10002209414/en/ (Accessed 28 January 2016), 1995.

768 Elzenga, J. T. M., Prins, H. B. A. and Stefels, J.: The role of extracellular carbonic anhydrase
769 activity in inorganic carbon utilization of *Phaeocystis globosa* (Prymnesiophyceae): A
770 comparison with other marine algae using the isotopic disequilibrium technique, , 45(2), 372–
771 380, 2000.

772 Engel, A., Schulz, K. G., Riebesell, U., Bellerby, R., Delille, B. and Schartau, M.: Effects of CO_2 on
773 particle size distribution and phytoplankton abundance during a mesocosm bloom experiment
774 (PeECE II), Biogeosciences, 5, 509–521, doi:10.5194/bgd-4-4101-2007, 2008.

775 Eppley, R. W.: Temperature and phytoplankton growth in the sea, Fish. Bull., 70(4), 1063–1085,
776 1972.

777 Errera, R. M., Yvon-Lewis, S., Kessler, J. D. and Campbell, L.: Reponses of the dinoflagellate
778 *Karenia brevis* to climate change: pCO_2 and sea surface temperatures, Harmful Algae, 37, 110–
779 116, doi:10.1016/j.hal.2014.05.012, 2014.

780 Feng, Y., Warner, M. E., Zhang, Y., Sun, J., Fu, F.-X., Rose, J. M. and Hutchins, D. A.: Interactive
781 effects of increased pCO_2 , temperature and irradiance on the marine coccolithophore *Emiliania*
782 *huxleyi* (Prymnesiophyceae), Eur. J. Phycol., 43(1), 87–98, doi:10.1080/09670260701664674,
783 2008.

784 Feng, Y., Hare, C., Leblanc, K., Rose, J., Zhang, Y., DiTullio, G., Lee, P., Wilhelm, S., Rowe, J., Sun, J.,
785 Nemcek, N., Gueguen, C., Passow, U., Benner, I., Brown, C. and Hutchins, D.A.: Effects of increased
786 pCO_2 and temperature on the North Atlantic spring bloom. I. The phytoplankton community and
787 biogeochemical response, Mar. Ecol. Prog. Ser., 388, 13–25, doi:10.3354/meps08133, 2009.

788 Flores-Moya, A., Rouco, M., García-Sánchez, M. J. S, García-Balboa, C., González, R., Costas, E. and
789 López-Rodas, V.: Effects of adaptation, chance, and history on the evolution of the toxic
790 dinoflagellate *Alexandrium minutum* under selection of increased temperature and acidification,
791 Ecol. Evol., 2(6), 1251–1259, doi:10.1002/ece3.198, 2012.

792 Fu, F., Tatters, A. and Hutchins, D. A: Global change and the future of harmful algal blooms in the
793 ocean, Mar. Ecol. Prog. Ser., 470, 207–233, doi:10.3354/meps10047, 2012.

794 Fu, F.-X., Warner, M. E., Zhang, Y., Feng, Y. and Hutchins, D. A.: Effects of Increased Temperature
795 and Co 2 on Photosynthesis, Growth, and Elemental Ratios in Marine *Synechococcus* and
796 *Prochlorococcus* (Cyanobacteria), J. Phycol., 43(3), 485–496, doi:10.1111/j.1529-
797 8817.2007.00355.x, 2007a.

798 Fu, F.-X., Zhang, Y., Warner, M. E., Feng, Y., Sun, J. and Hutchins, D. A.: A comparison of future

799 increased CO_2 and temperature effects on sympatric *Heterosigma akashiwo* and *Prorocentrum*
800 *minimum*, Harmful Algae, 7(1), 76–90, doi:10.1016/j.hal.2007.05.006, 2008.

801 Fu, F. X., Place, A. R., Garcia, N. S. and Hutchins, D. A.: CO_2 and phosphate availability control the
802 toxicity of the harmful bloom dinoflagellate *Karlodinium veneficum*, Aquat. Microb. Ecol., 59(1),
803 55–65, doi:10.3354/ame01396, 2010.

804 Gao, G., Jin, P., Liu, N., Li, F., Tong, S., Hutchins, D. A. and Gao, K.: The acclimation process of
805 phytoplankton biomass, carbon fixation and respiration to the combined effects of elevated
806 temperature and pCO_2 in the northern South China Sea, Mar. Pollut. Bull., 118(1–2), 213–220,
807 doi:10.1016/j.marpolbul.2017.02.063, 2017.

808 Giordano, M., Beardall, J. and Raven, J. A: CO_2 concentrating mechanisms in algae: mechanisms,
809 environmental modulation, and evolution., Annu. Rev. Plant Biol., 56(January), 99–131,
810 doi:10.1146/annurev.arplant.56.032604.144052, 2005.

811 Goldman, J. and Carpenter, E.: A kinetic approach to the effect of temperature on algal growth,
812 Limnol. Oceanogr., 19(5), 756–766, doi:10.4319/lo.1974.19.5.0756, 1974.

813 Grzebyk, D., Denardou, A, Berland, B. and Pouchus, Y. F.: Evidence for a new toxin in the red-tide
814 dinoflagellate *Prorocentrum minimum*, J. Plankton Res., 19(8), 1111–1124,
815 doi:10.1093/plankt/19.8.1111, 1997.

816 Hajdu, S., Edler, L., Olenina, I. and Witek, B.: Spreading and establishment of the potentially toxic
817 dinoflagellate *Prorocentrum minimum* in the Baltic Sea, Int. Rev. Hydrobiol., 85(5–6), 561–575,
818 doi:10.1002/1522-2632(200011)85:5/6<561::AID-IROH561>3.0.CO;2-3, 2000.

819 Hallegraeff, G. M.: A review of harmful algal blooms and their apparent global increase,
820 Phycologia, 32(2), 79–99, doi:10.2216/i0031-8884-32-2-79.1, 1993.

821 Hansen, P.: Effect of high pH on the growth and survival of marine phytoplankton: implications
822 for species succession, Aquat. Microb. Ecol., 28, 279–288, doi:10.3354/ame028279, 2002.

823 Hare, C., Leblanc, K., DiTullio, G., Kudela, R., Zhang, Y., Lee, P., Riseman, S. and Hutchins, D. A.:
824 Consequences of increased temperature and CO_2 for phytoplankton community structure in the
825 Bering Sea, Mar. Ecol. Prog. Ser., 352, 9–16, doi:10.3354/meps07182, 2007.

826 Harris, R.: The L4 time-series: the first 20 years, J. Plankton Res., 32(5), 577–583,
827 doi:10.1093/plankt/fbq021, 2010.

828 Heil, C. A., Glibert, P. M. and Fan, C.: *Prorocentrum minimum* (Pavillard) Schiller: A review of a
829 harmful algal bloom species of growing worldwide importance, Harmful Algae, 4(3), 449–470,

doi:10.1016/j.hal.2004.08.003, 2005.

Herberich, E., Sikorski, J. and Hothorn, T.: A Robust Procedure for Comparing Multiple Means under Heteroscedasticity in Unbalanced Designs, PLoS One, 5(3), e9788, doi:10.1371/journal.pone.0009788, 2010.

Hinga, K. R.: Effects of pH on coastal marine phytoplankton, Mar. Ecol. Prog. Ser., 238, 281–300, 2002.

Hoogstraten, A., Peters, M., Timmermans, K. R. and De Baar, H. J. W.: Combined effects of inorganic carbon and light on *Phaeocystis globosa* Scherffel (Prymnesiophyceae), Biogeosciences, 9(5), 1885–1896, doi:10.5194/bg-9-1885-2012, 2012.

Hutchins, D. A., Fu, F.-X., Zhang, Y., Warner, M. E., Feng, Y., Portune, K., Bernhardt, P. W. and Mulholland, M. R.: CO_2 control of *Trichodesmium* N2 fixation, photosynthesis, growth rates, and elemental ratios: Implications for past, present, and future ocean biogeochemistry, Limnol. Oceanogr., 52(4), 1293–1304, doi:10.4319/lo.2007.52.4.1293, 2007.

Keys, M., Tilstone, G., Findlay, H. S., Widdicombe, C. E. and Lawson, T.: Effects of elevated CO_2 on phytoplankton community biomass and species composition during a spring *Phaeocystis* spp. bloom in the western English Channel, Harmful Algae, 67, 92–106, doi:10.1016/j.hal.2017.06.005, 2017.

Kiefer, D. A. and Mitchell, B. G.: A simple steady state description of phytoplankton growth based on absorption cross section and quantum efficiency, Limnol. Oceanogr., 28(4), 770–776, doi:10.4319/lo.1983.28.4.0770, 1983.

Kim, J.-M., Lee, K., Shin, K., Kang, J.-H., Lee, H.-W., Kim, M., Jang, P.-G. and Jang, M.-C.: The effect of seawater CO_2 concentration on growth of a natural phytoplankton assemblage in a controlled mesocosm experiment, Limnol. Oceanogr., 51(4), 1629–1636, doi:10.4319/lo.2006.51.4.1629, 2006.

Kitidis, V., Hardman-mountford, N. J., Litt, E., Brown, I., Cummings, D., Hartman, S., Hydes, D., Fishwick, J. R., Harris, C., Martinez-vicente, V., Woodward, E. M. S. and Smyth, T. J.: Seasonal dynamics of the carbonate system in the Western English Channel, Cont. Shelf Res., 42, 2–12, 2012.

Kolber, Z. S., Prášil, O. and Falkowski, P. G.: Measurements of variable chlorophyll fluorescence using fast repetition rate techniques: Defining methodology and experimental protocols, Biochim. Biophys. Acta - Bioenerg., 1367(1–3), 88–106, doi:10.1016/S0005-2728(98)00135-2, 1998.

862 Kovala, P. E. and Larrance, J. D.: COMPUTATION OF PHYTOPLANKTON CELL NUMBERS, CELL
863 VOLUME, CELL SURFACE AND PLASMA VOLUME PER LITER, FROM MICROSCOPICAL COUNTS.,
864 DTIC Document., 1966.

865 Laws, E. A., Falkowski, P. G., Smith, W. O., Ducklow, H. W. and McCarthy, J. J.: Temperature effects
866 on export production in the open ocean, Global Biogeochem. Cycles, 14(4), 1231–1246,
867 doi:10.1029/1999GB001229, 2000.

868 Li, W. K. W., McLaughlin, F. A., Lovejoy, C. and Carmack, E. C.: Smallest Algae Thrive As the Arctic
869 Ocean Freshens, Science (80-.)., 326(5952), 539–539, doi:10.1126/science.1179798, 2009.

870 Lomas, M. W. and Glibert, P. M.: Interactions between NH_4/+ and NO_3/- uptake and assimilation:
871 Comparison of diatoms and dinoflagellates at several growth temperatures, Mar. Biol., 133(3),
872 541–551, doi:10.1007/s002270050494, 1999.

873 Love, B. A., Olson, M. B. and Wuori, T.: Technical Note: A minimally-invasive experimental
874 system for pCO_2 manipulation in plankton cultures using passive gas exchange (Atmospheric
875 Carbon Control Simulator), Biogeosciences Discuss., (December), 1–19, doi:10.5194/bg-2016-
876 502, 2016.

877 Maugendre, L., Gattuso, J. P., Poulton, A. J., Dellisanti, W., Gaubert, M., Guieu, C. and Gazeau, F.: No
878 detectable effect of ocean acidification on plankton metabolism in the NW oligotrophic
879 Mediterranean Sea: Results from two mesocosm studies, Estuar. Coast. Shelf Sci., 186, 89–99,
880 doi:10.1016/j.ecss.2015.03.009, 2017.

881 Mehrbach, C., Culberson, C. H., Hawley, J. E. and Pytkowicz, R. M.: Measurement of the Apparent
882 Dissociation Constants of Carbonic Acid in Seawater at Atmospheric Pressure, Limnol.
883 Oceanogr., 18(1932), 897–907, 1973.

884 Menden-Deuer, S. and Lessard, E. J.: Carbon to volume relationships for dinoflagellates, diatoms,
885 and other protist plankton, Limnol. Oceanogr., 45(3), 569–579, doi:10.4319/lo.2000.45.3.0569,
886 2000.

887 Morán, X. A. G., López-Urrutia, Á., Calvo-Díaz, A. and Li, W. K. W.: Increasing importance of small
888 phytoplankton in a warmer ocean, Glob. Chang. Biol., 16(3), 1137–1144, doi:10.1111/j.1365-
889 2486.2009.01960.x, 2010.

890 Morse, D., Salois, P., Markovic, P. and Hastings, J. W.: A nuclear-encoded form II RuBisCO in
891 dinoflagellates., Science, 268(5217), 1622–1624, doi:10.1126/science.7777861, 1995.

892 Moustaka-Gouni, M., Kormas, K. A., Scotti, M., Vardaka, E. and Sommer, U.: Warming and
893 Acidification Effects on Planktonic Heterotrophic Pico- and Nanoflagellates in a Mesocosm

Experiment, Protist, 167(4), 389–410, doi:10.1016/j.protis.2016.06.004, 2016.

Oxborough, K., Moore, C. M., Suggett, D. J., Lawson, T., Chan, H. G. and Geider, R. J.: Direct estimation of functional PSII reaction center concentration and PSII electron flux on a volume basis: a new approach to the analysis of Fast Repetition Rate fluorometry (FRRf) data, Limnol. Oceanogr. Methods, 10, 142–154, doi:10.4319/lom.2012.10.142, 2012.

Paul, C., Matthiessen, B. and Sommer, U.: Warming, but not enhanced CO_2 concentration, quantitatively and qualitatively affects phytoplankton biomass, Mar. Ecol. Prog. Ser., 528, 39–51, doi:10.3354/meps11264, 2015.

Paulino, A. I., Egge, J. K. and Larsen, A.: Effects of increased atmospheric CO_2 on small and intermediate sized osmotrophs during a nutrient induced phytoplankton bloom, Biogeosciences Discuss., 4(6), 4173–4195, doi:10.5194/bgd-4-4173-2007, 2007.

Peter, K. H. and Sommer, U.: Phytoplankton Cell Size: Intra- and Interspecific Effects of Warming and Grazing, PLoS One, 7(11), doi:10.1371/journal.pone.0049632, 2012.

Pierrot, D., Lewis, E. and Wallace, D. W. R.: MS Excel program developed for CO_2 system calculations, ORNL/CDIAC-105a. Carbon Dioxide Inf. Anal. Center, Oak Ridge Natl. Lab. US Dep. Energy, Oak Ridge, Tennessee, 2006.

Raupach, M. R., Marland, G., Ciais, P., Le Quéré, C., Canadell, J. G., Klepper, G. and Field, C. B.: Global and regional drivers of accelerating CO_2 emissions., Proc. Natl. Acad. Sci. U. S. A., 104(24), 10288–93, doi:10.1073/pnas.0700609104, 2007.

Raven. J. A., Caldeira. K., Elderfield. H., H.-G. and others: Ocean acidification due to increasing atmospheric carbon dioxide, R. Soc., (June), 2005.

Raven, J. A. and Geider, R. J.: Temperature and algal growth, New Phytol., 110(4), 441–461, doi:10.1111/j.1469-8137.1988.tb00282.x, 1988.

Reinfelder, J. R.: Carbon Concentrating Mechanisms in Eukaryotic Marine Phytoplankton, Ann. Rev. Mar. Sci., 3(1), 291–315, doi:10.1146/annurev-marine-120709-142720, 2011.

Riebesell, U.: Effects of CO_2 Enrichment on Marine Phytoplankton, J. Oceanogr., 60(4), 719–729, doi:10.1007/s10872-004-5764-z, 2004.

Riebesell, U., Schulz, K. G., Bellerby, R. G. J., Botros, M., Fritsche, P., Meyerhöfer, M., Neill, C., Nondal, G., Oschlies, a, Wohlers, J. and Zöllner, E.: Enhanced biological carbon consumption in a high CO_2 ocean., Nature, 450(7169), 545–8, doi:10.1038/nature06267, 2007.

Riebesell, U., Fabry, V. J., Hansson, L. and Gattuso, J.-P.: Guide to best practices for ocean

925 acidification, edited by L. H. and J. –P. G. L. U. Riebesell, V. J. Fabry, Publications Office Of The
926 European Union., 2010.

927 Rost, B., Riebesell, U., Burkhardt, S. and Su, D.: Carbon acquisition of bloom-forming marine
928 phytoplankton, Limnol. Oceanogr., 48(1), 55–67, 2003.

929 Savage, V. M., Gillooly, J. F., Brown, J. H., West, G. B. and Charnov, E. L.: Effects of Body Size and
930 Temperature on Population Growth, Am. Nat., 163(3), 429–441, doi:10.1086/381872, 2004.

931 Schoemann, V., Becquevort, S., Stefels, J., Rousseau, V. and Lancelot, C.: *Phaeocystis* blooms in the
932 global ocean and their controlling mechanisms: a review, J. Sea Res., 53(1–2), 43–66,
933 doi:10.1016/j.seares.2004.01.008, 2005.

934 Schulz, K. G., Ramos, J. B., Zeebe, R. E. and Riebesell, U.: Biogeosciences CO_2 perturbation
935 experiments : similarities and differences between dissolved inorganic carbon and total
936 alkalinity manipulations, Biogeosciences, 6, 2145–2153, 2009.

937 Shi, D., Xu, Y. and Morel, F. M. M.: Effects of the pH/pCO_2 control method on medium chemistry
938 and phytoplankton growth, Biogeosciences, 6(7), 1199–1207, doi:10.5194/bg-6-1199-2009,
939 2009.

940 Smetacek, V. and Cloern, J. E.: On Phytoplankton Trends, Science (80-.)., 319(5868), 1346–1348
941 [online] Available from: http://www.jstor.org/stable/20053523, 2008.

942 Smyth, T. J., Fishwick, J. R., AL-Moosawi, L., Cummings, D. G., Harris, C., Kitidis, V., Rees, A.,
943 Martinez-Vicente, V. and Woodward, E. M. S.: A broad spatio-temporal view of the Western
944 English Channel observatory, J. Plankton Res., 32(5), 585–601, doi:10.1093/plankt/fbp128,
945 2010.

946 Stoecker, D. K., Li, A. S., Coats, D. W., Gustafson, D. E. and Nannen, M. K.: Mixotrophy in the
947 dinoflagellate *Prorocentrum minimum*, Mar. Ecol. Prog. Ser., 152(1–3), 1–12,
948 doi:10.3354/meps152001, 1997.

949 Sun, J., Hutchins, D. A., Seubert, E. L., Feng, Y., Caron, D. A. and Fu, F.-X.: Effects of changing pCO_2
950 and phosphate availability on domoic acid production and physiology of the marine harmful
951 bloom diatom *Pseudo-nitzschia multiseries*, Limnol. Oceanogr., 56, 829–840,
952 doi:10.4319/lo.2011.56.3.0829, 2011.

953 Tango, P. J., Magnien, R., Butler, W., Luckett, C., Luckenbach, M., Lacouture, R. and Poukish, C.:
954 Impacts and potential effects due to *Prorocentrum minimum* blooms in Chesapeake Bay,
955 Harmful Algae, 4(3), 525–531, doi:10.1016/j.hal.2004.08.014, 2005.

956 Tarran, G. A., Heywood, J. L. and Zubkov, M. V.: Latitudinal changes in the standing stocks of
957 nano- and picoeukaryotic phytoplankton in the Atlantic Ocean, Deep Sea Res. Part II Top. Stud.
958 Oceanogr., 53(14–16), 1516–1529, doi:10.1016/j.dsr2.2006.05.004, 2006.

959 Tatters, A. O., Fu, F. X. and Hutchins, D. A.: High CO_2 and silicate limitation synergistically
960 increase the toxicity of *Pseudo-nitzschia fraudulenta*, PLoS One, 7(2),
961 doi:10.1371/journal.pone.0032116, 2012.

962 Taucher, J., Jones, J., James, A., Brzezinski, M. A., Carlson, C. A., Riebesell, U. and Passow, U.:
963 Combined effects of CO_2 and temperature on carbon uptake and partitioning by the marine
964 diatoms *Thalassiosira weissflogii* and *Dactyliosolen fragilissimus*, Limnol. Oceanogr., 60(3), 901–
965 919, doi:10.1002/lno.10063, 2015.

966 Thoisen, C., Riisgaard, K., Lundholm, N., Nielsen, T. and Hansen, P.: Effect of acidification on an
967 Arctic phytoplankton community from Disko Bay, West Greenland, Mar. Ecol. Prog. Ser., 520,
968 21–34, doi:10.3354/meps11123, 2015.

969 Thomas, M. K., Kremer, C. T., Klausmeier, C. A. and Litchman, E.: A Global Pattern of Thermal
970 Adaptation in Marine Phytoplankton, Science (80-.)., 338(6110), 1085–1088,
971 doi:10.1126/science.1224836, 2012.

972 Torstensson, A., Chierici, M. and Wulff, A.: The influence of increased temperature and carbon
973 dioxide levels on the benthic/sea ice diatom *Navicula directa*, Polar Biol., 35(2), 205–214,
974 doi:10.1007/s00300-011-1056-4, 2012.

975 Tortell, P., DiTullio, G., Sigman, D. and Morel, F.: CO_2 effects on taxonomic composition and
976 nutrient utilization in an Equatorial Pacific phytoplankton assemblage, Mar. Ecol. Prog. Ser., 236,
977 37–43, doi:10.3354/meps236037, 2002.

978 Tortell, P. D., Payne, C. D., Li, Y., Trimborn, S., Rost, B., Smith, W. O., Riesselman, C., Dunbar, R. B.,
979 Sedwick, P. and DiTullio, G. R.: CO_2 sensitivity of Southern Ocean phytoplankton, Geophys. Res.
980 Lett., 35(4), L04605, doi:10.1029/2007GL032583, 2008.

981 Utermöhl, H.: Zur vervollkommnung der quantitativen phytoplankton-methodik, Mitt. int. Ver.
982 theor. angew. Limnol., 9, 1–38, 1958.

983 Verity, P. G., Brussaard, C. P., Nejstgaard, J. C., Van Leeuwe, M. a., Lancelot, C. and Medlin, L. K.:
984 Current understanding of *Phaeocystis* ecology and biogeochemistry, and perspectives for future
985 research, edited by M. A. van Leeuwe, J. Stefels, S. Belviso, C. Lancelot, P. G. Verity, and W. W. C.
986 Gieskes, Springer Netherlands., 2007.

987 Vlamis, A., Katikou, P., Rodriguez, I., Rey, V., Alfonso, A., Papazachariou, A., Zacharaki, T., Botana,

A. M. and Botana, L. M.: First detection of tetrodotoxin in greek shellfish by UPLC-MS/MS potentially linked to the presence of the dinoflagellate *Prorocentrum minimum*, Toxins (Basel)., 7(5), 1779–1807, doi:10.3390/toxins7051779, 2015.

Webb, W. L., Newton, M. and Starr, D.: Carbon dioxide exchange of *Alnus rubra*, Oecologia, 17(4), 281–291, doi:10.1007/BF00345747, 1974.

Welschmeyer: Fluorometric analysis of chlorophyll a in the presence of chlorophyll b and pheopigments, Limnol. Oceanogr., 39(8), 1985–1992, 1994.

Widdicombe, C. E., Eloire, D., Harbour, D., Harris, R. P. and Somerfield, P. J.: Long-term phytoplankton community dynamics in the Western English Channel, J. Plankton Res., 32(5), 643–655, doi:10.1093/plankt/fbp127, 2010.

Wolf-gladrow, B. D. A., Riebesell, U. L. F., Burkhardt, S. and Jelle, B.: Direct effects of CO_2 concentration on growth and isotopic composition of marine plankton, Tellus, 51B, 461–476, 1999.

Woods, H. A. and Harrison, J. F.: Temperature and the chemical composition of poikilothermic organisms, (Sidell 1998), 237–245, 2003.

Biogeosciences Discuss., https://doi.org/10.5194/bg-2017-510
Manuscript under review for journal Biogeosciences
Discussion started: 4 December 2017

.015

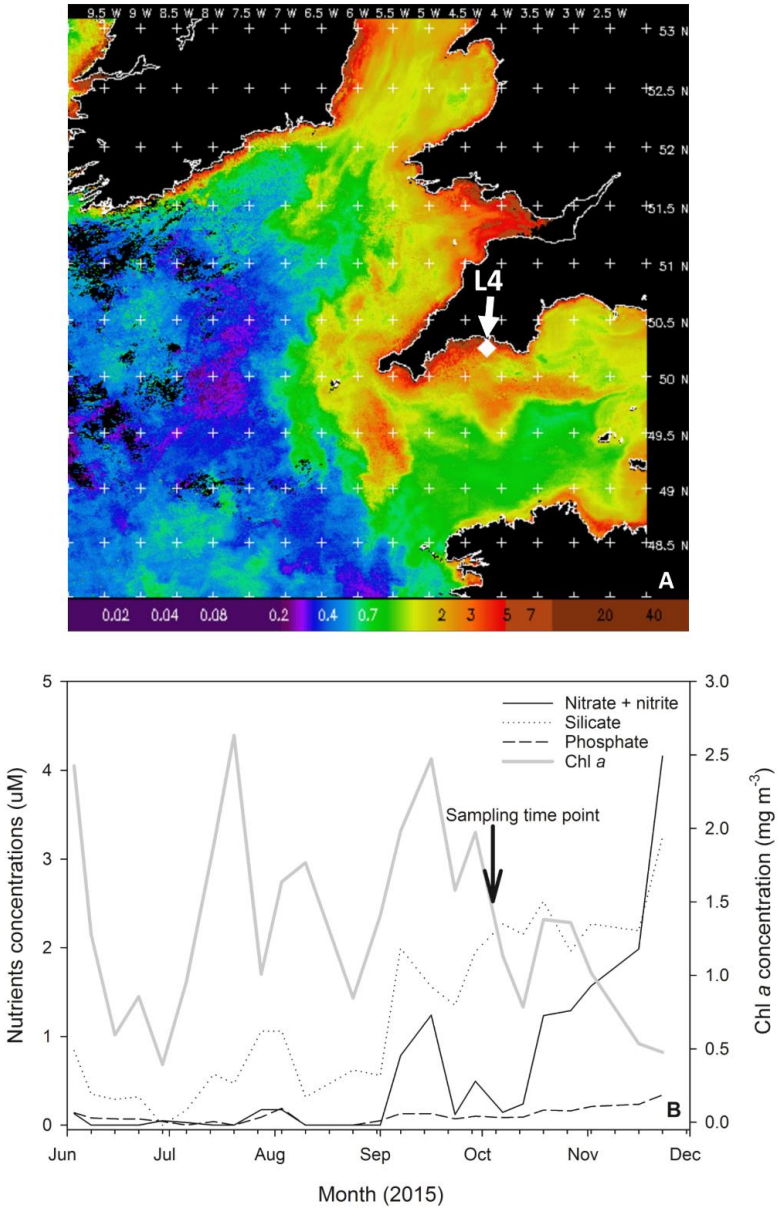

Fig. 1. (**A**). MODIS weekly composite chl *a* image of the western English Channel covering the period 30th September – 6th October 2015 (coincident with the week of phytoplankton community sampling for the present study), processing courtesy of NEODAAS. The position of coastal station L4 is marked with a white diamond. (**B**). Profiles of weekly nutrient and chl *a* concentrations from station L4 at a depth of 10 m over the second half of 2015 in the months prior to phytoplankton community sampling (indicated by black arrow and text).

.016

Biogeosciences Discuss., https://doi.org/10.5194/bg-2017-510
Manuscript under review for journal Biogeosciences
Discussion started: 4 December 2017

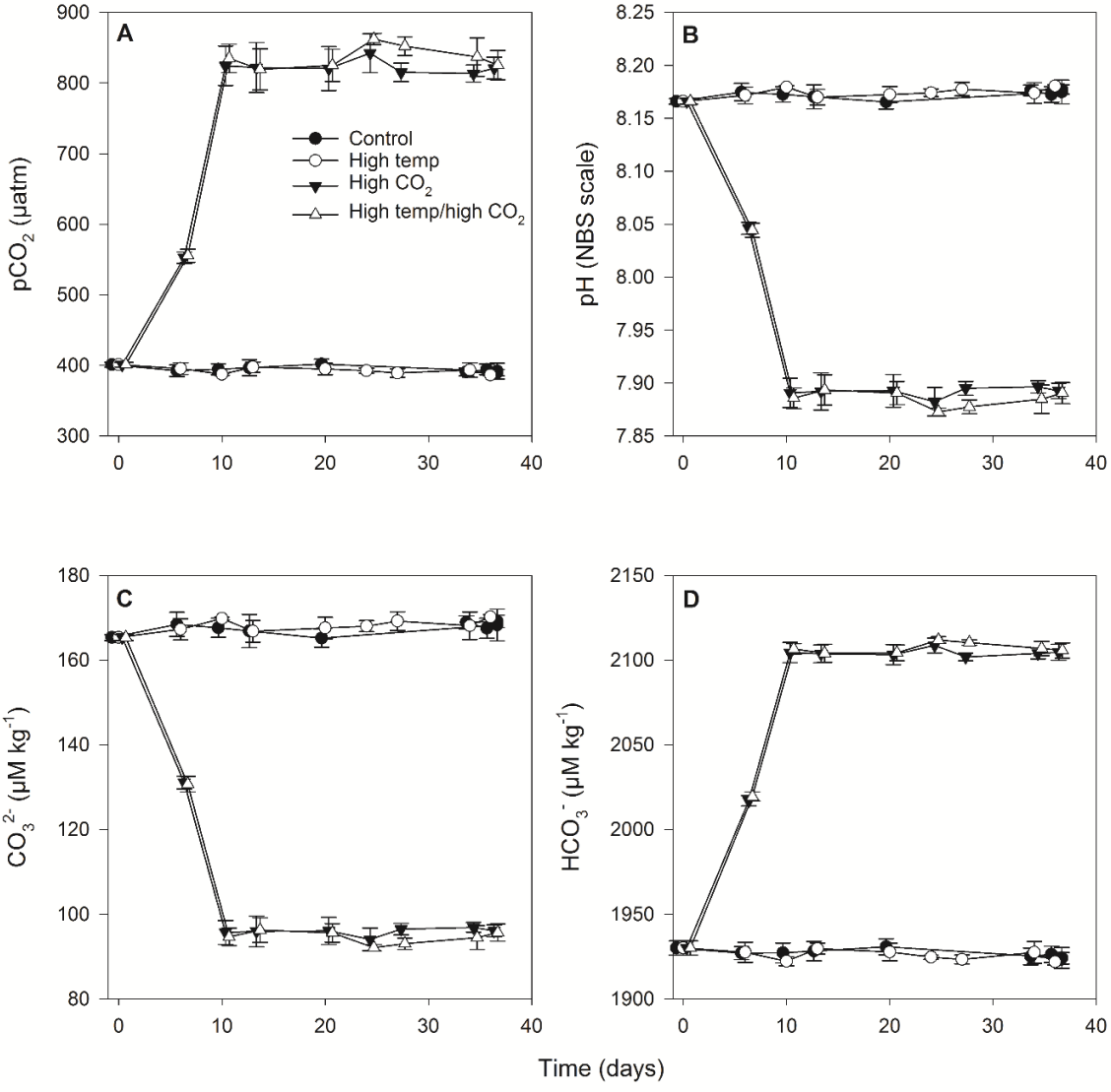

Fig. 2. Carbonate system values of the experimental phytoplankton incubations. (**A**). partial pressure of CO_2 in seawater (pCO_2), (**B**). pH on the NBS scale, (**C**). carbonate concentration (CO_3^{2-}) and (**D**). bicarbonate concentration (HCO_3^-) were estimated from direct measurements of total alkalinity and dissolved inorganic carbon.

Biogeosciences Discuss., https://doi.org/10.5194/bg-2017-510
Manuscript under review for journal Biogeosciences
Discussion started: 4 December 2017

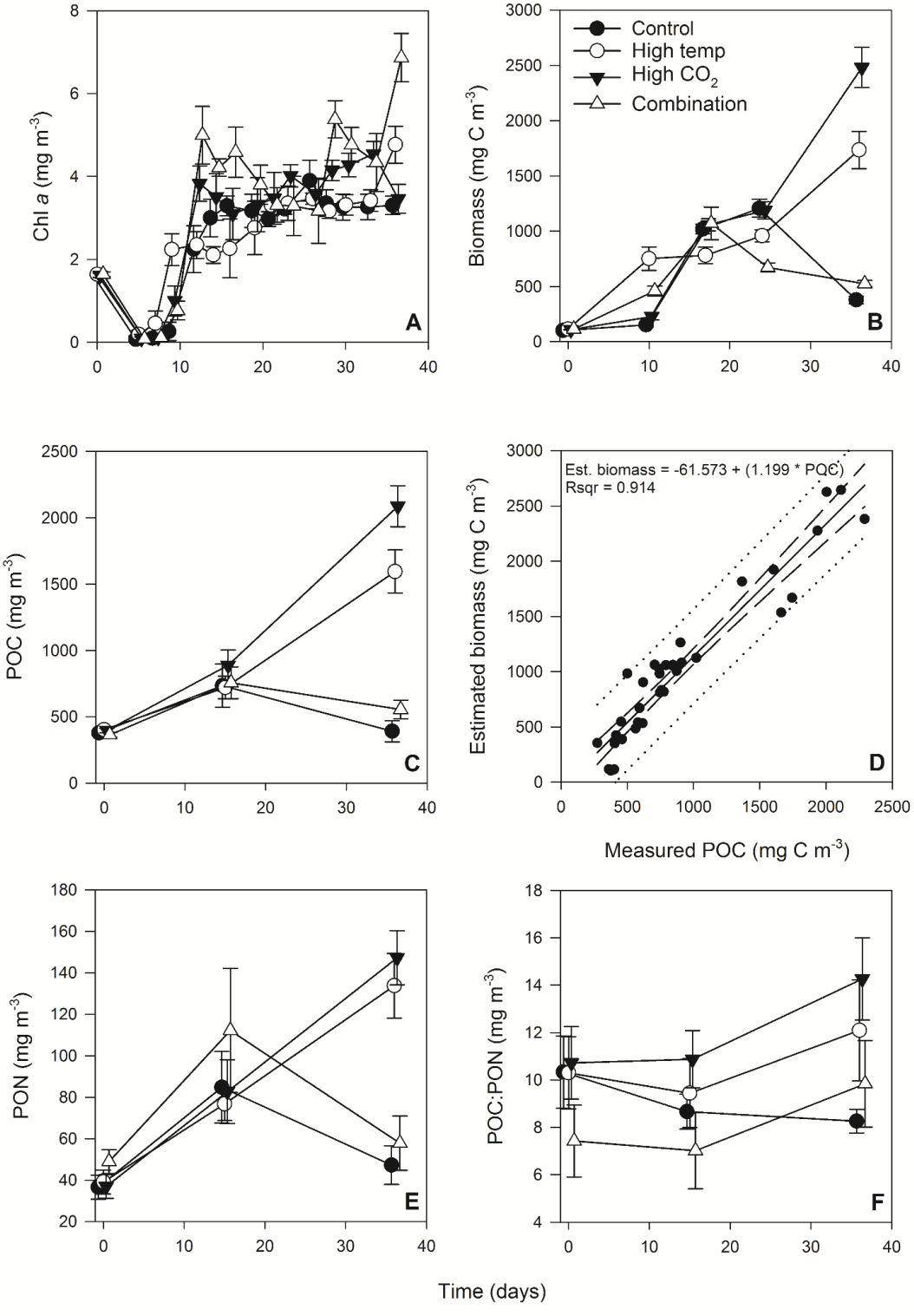

Fig. 3. Time course of chl *a* (**A**), estimated phytoplankton biomass (**B**), POC (**C**), regression of estimated phytoplankton carbon vs measured POC (**D**), PON (**E**) and POC:PON (**F**).

Biogeosciences Discuss., https://doi.org/10.5194/bg-2017-510
Manuscript under review for journal Biogeosciences
Discussion started: 4 December 2017

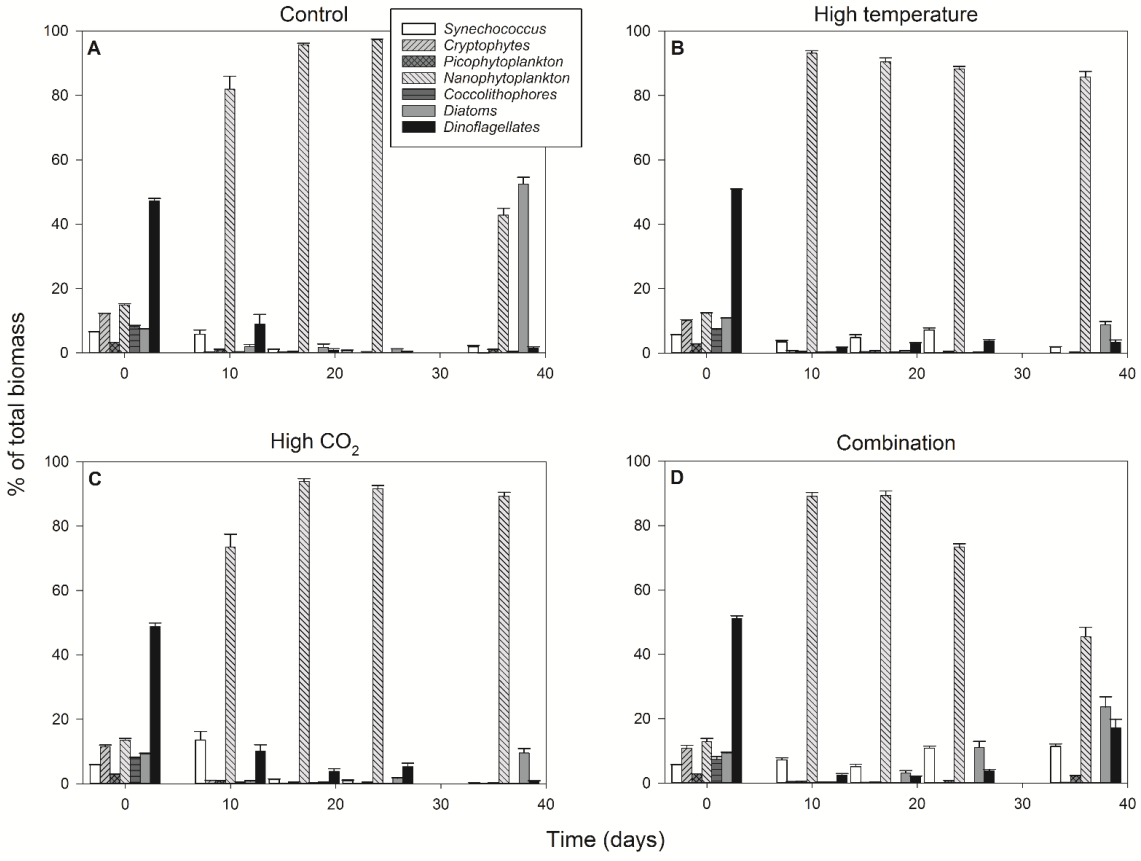

Fig. 4. Percentage contribution to community biomass by phytoplankton groups/species throughout the experiment in the control (**A**), high temperature (**B**), high CO_2 (**C**) and combination treatments (**D**).

Biogeosciences Discuss., https://doi.org/10.5194/bg-2017-510
Manuscript under review for journal Biogeosciences
Discussion started: 4 December 2017

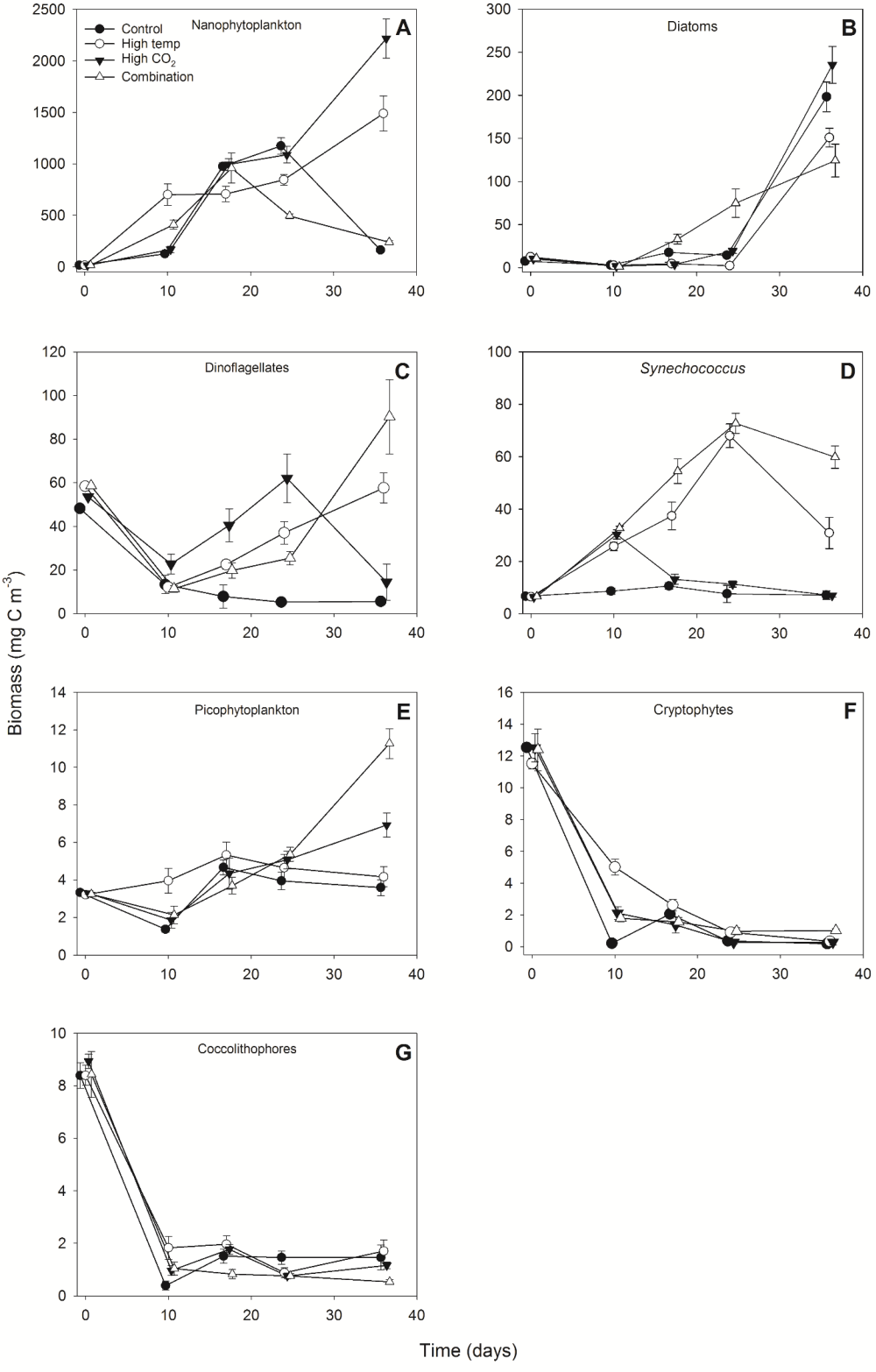

Fig. 5. Response of individual phytoplankton groups to experimental treatments.

Biogeosciences Discuss., https://doi.org/10.5194/bg-2017-510
Manuscript under review for journal Biogeosciences
Discussion started: 4 December 2017

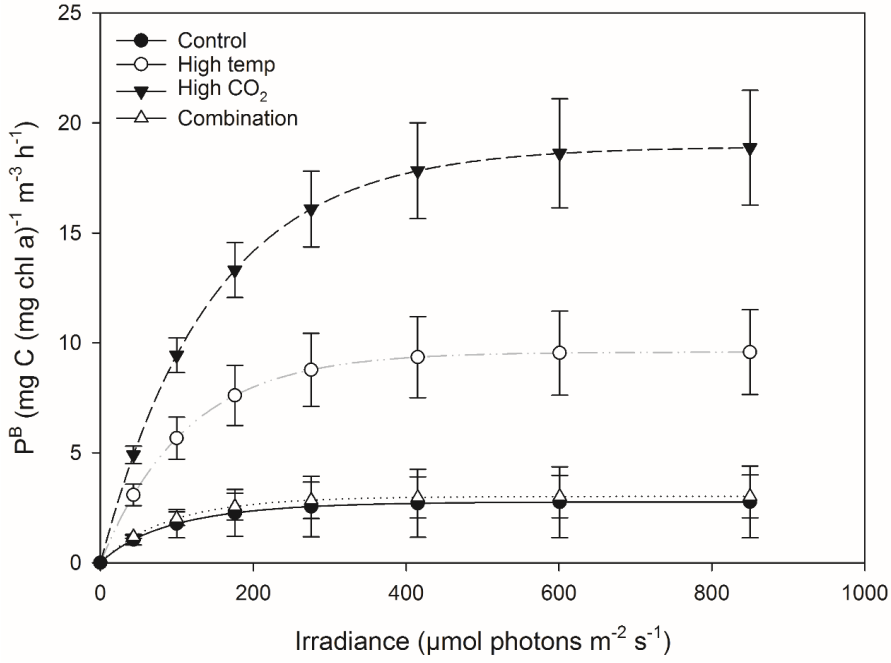

Fig. 6. Fitted parameters of FRRf-based photosynthesis-irradiance curves for the experimental treatments on the final experimental day (T36)

Biogeosciences Discuss., https://doi.org/10.5194/bg-2017-510
Manuscript under review for journal Biogeosciences
Discussion started: 4 December 2017

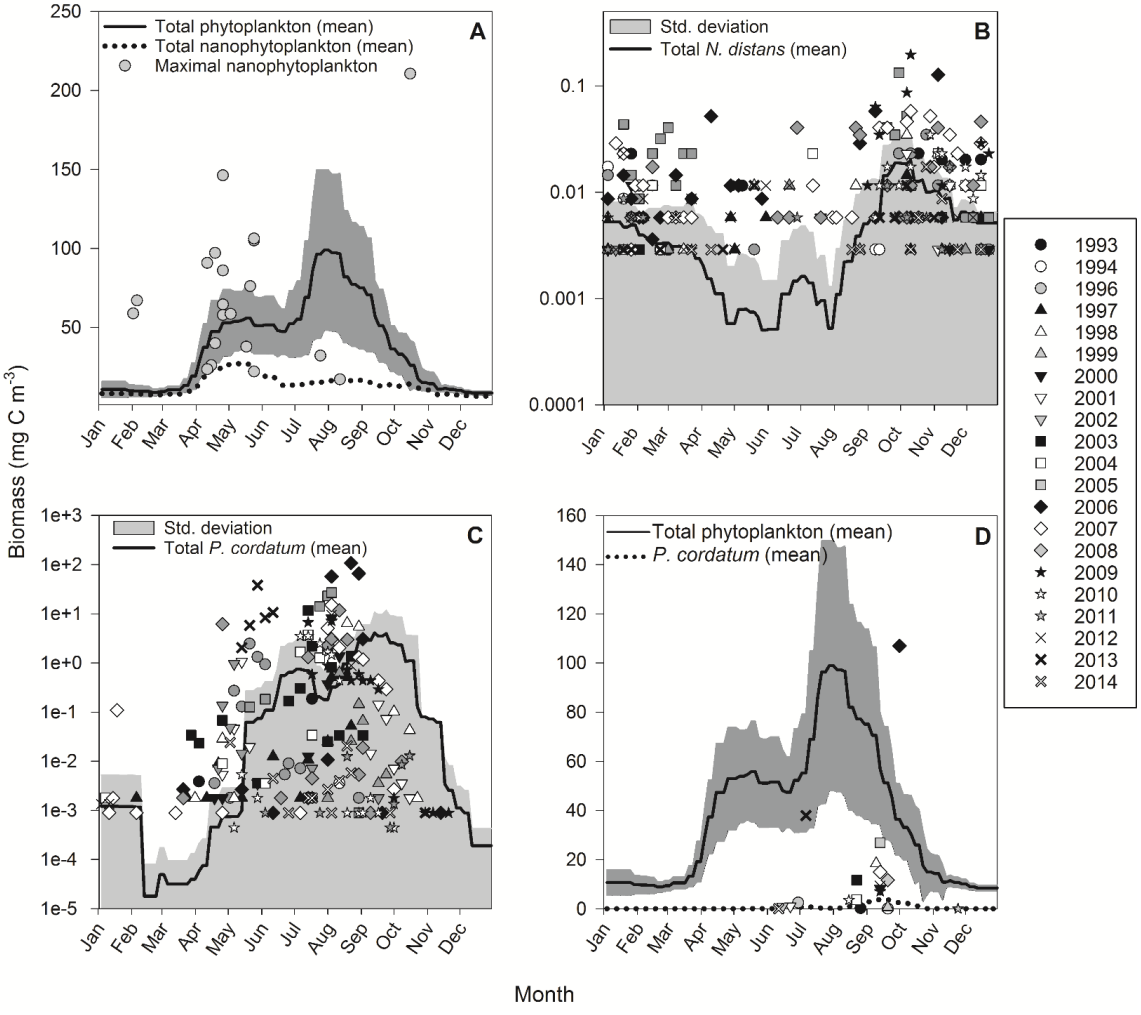

Fig. 7. (**A**) Temporal weekly profile of total phytoplankton carbon biomass at station L4 between 1993-2014. Black line is smoothed running average of total phytoplankton, grey area is standard deviation, dotted line is smoothed running average of total nanophytoplankton biomass and grey circles are maximal nanophytoplankton biomass from weekly observations (mean maxima of 70 mg C m^{-3}). (**B**) Seasonal profiles of *Navicula distans* (common log scale) between 1993-2014. Black line is smoothed running average over the time series, grey area is standard deviation and all symbols are observed data values by year. (**C**) Seasonal profiles of *Prorocentrum cordatum* (common log scale) between 1993-2014. Black line is smoothed running average over the time series, grey area is standard deviation and all symbols are observed data values by year. (**D**)Maximal *P. cordatum* biomass values relative to total phytoplankton biomass. Black line is smoothed running average of total phytoplankton biomass, grey area is standard deviation, dotted line is mean *P. cordatum* biomass and symbols are maximal *P. cordatum* biomass from weekly observations by year (as per figure legend for **B & C.**).

Biogeosciences Discuss., https://doi.org/10.5194/bg-2017-510
Manuscript under review for journal Biogeosciences
Discussion started: 4 December 2017

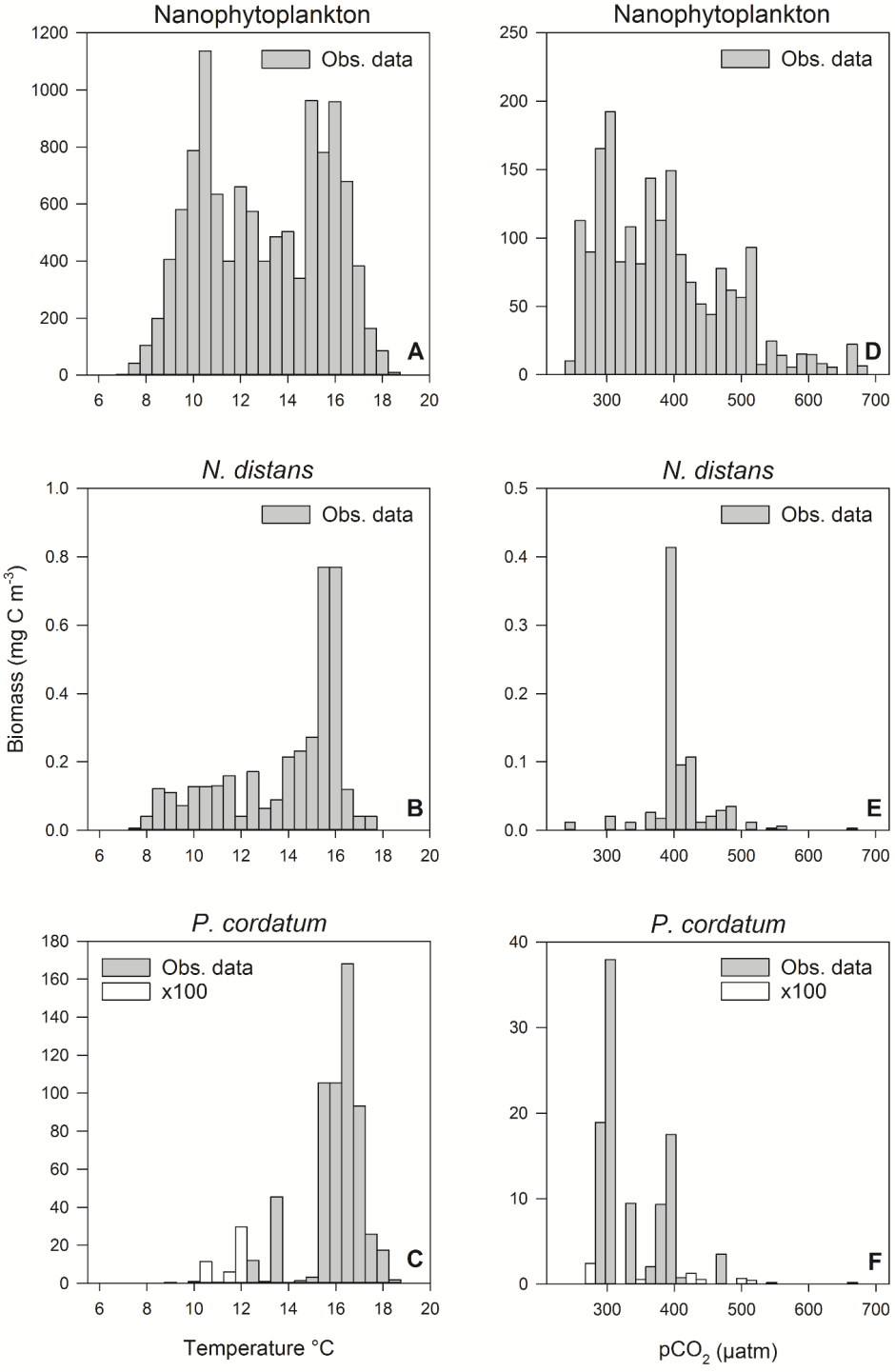

Fig. 8. Frequency distribution of biomass at station L4 along the *in-situ* gradients of temperature (1993-2014) and pCO_2 (2008-2014) for nanophytoplankton (**A & D**) *N. distans* (**B & E**) and *P. cordatum* (**C & F**).

.044

Biogeosciences Discuss., https://doi.org/10.5194/bg-2017-510
Manuscript under review for journal Biogeosciences
Discussion started: 4 December 2017

Table 1. Results of generalised least-squares model testing for main effects of time, high temperature, high CO_2 and all interactions on chl *a*, phytoplankton biomass and particulate organic nitrogen. Significant results are in bold; * p < 0.05, ** p < 0.001, *** p < 0.0001.

Response variable	n	*df*	*t*-value	*p*	sig
Chla (mg m^{-3})					
Time	80	72	3.782211	**0.0003**	**
High temp	80	72	0.688339	0.4935	
High CO_2	80	72	0.765811	0.4463	
Time x high temp	80	72	0.330431	0.742	
Time x high CO_2	80	72	-0.596962	0.5524	
High temp x high CO_2	80	72	0.338096	0.7363	
Time x high temp x high CO_2	80	72	1.302498	0.1969	
Estimated biomass (mg C m^{-3})					
Time	80	72	3.339498	**0.0013**	*
High temp	80	72	-0.144359	0.8856	
High CO_2	80	72	-1.008942	0.3164	
Time x high temp	80	72	3.189888	**0.0021**	*
Time x high CO_2	80	72	4.751901	**0.0000**	***
High temp x high CO_2	80	72	0.341905	0.7334	
Time x high temp x high CO_2	80	72	0.449075	0.6547	
POC (mg m^{-3})					
Time	48	40	-0.27037	0.7883	
High temp	48	40	-1.2607	0.2147	
High CO_2	48	40	-1.13796	0.2619	
Time x high temp	48	40	5.31006	**0.0000**	***
Time x high CO_2	48	40	6.24182	**0.0000**	***
High temp x high CO_2	48	40	-0.38194	0.7045	
Time x high temp x high CO_2	48	40	1.21692	0.2308	
PON (mg m^{-3})					
Time	48	40	0.276438	0.7836	
High temp	48	40	-1.447791	0.1555	
High CO_2	48	40	-1.571726	0.1239	
Time x high temp	48	40	4.78625	**0.0000**	***
Time x high CO_2	48	40	5.493647	**0.0000**	***
High temp x high CO_2	48	40	0.95334	0.3461	
Time x high temp x high CO_2	48	40	-0.126291	0.9001	
POC:PON (mg m^{-3})					
Time	48	40	-3.248155	**0.0024**	*
High temp	48	40	-0.206777	0.8372	
High CO_2	48	40	-0.055976	0.9556	
Time x high temp	48	40	2.433457	**0.0195**	*
Time x high CO_2	48	40	3.838128	**0.0004**	***
High temp x high CO_2	48	40	-2.932253	**0.0055**	*
Time x high temp x high CO_2	48	40	2.40294	**0.021**	*

Biogeosciences Discuss., https://doi.org/10.5194/bg-2017-510
Manuscript under review for journal Biogeosciences
Discussion started: 4 December 2017

Table 2. Results of generalised linear model testing for significant effects of temperature, CO_2 and temperature x CO_2 on chl *a* and phytoplankton biomass at the experiment end (T36). Significant results are in bold; * p < 0.05, ** p < 0.001, *** p < 0.0001.

Response variable	n	*df*	*z*-value	*p*	sig
Chl *a* mg m^{-3}					
High temp	16	12	7.413	**< 0.0001**	***
High CO_2	16	12	0.804	0.437	
High temp x high CO_2	16	12	18.043	**<0.0001**	***
Total biomass (mg C m^{-3})					
High temp	16	12	28.953	**< 0.0001**	***
High CO_2	16	12	36.042	**< 0.0001**	***
High temp x high CO_2	16	12	5.899	**< 0.0001**	***
Diatoms (mg C m^{-3})					
High temp	16	12	-4.43	**<0.0001**	***
High CO_2	16	12	3.036	**0.0024**	**
High temp x high CO_2	16	12	-7.243	**<0.0001**	***
Dinoflagellates (mg C m^{-3})					
High temp	16	12	9.848	**<0.0001**	***
High CO_2	16	12	1.805	0.2927	
High temp x high CO_2	16	12	11.902	**<0.0001**	***
Nanophytoplankton (mg m^{-3})					
High temp	16	12	32.9	**<0.0001**	***
High CO_2	16	12	39.04	**<0.0001**	***
High temp x high CO_2	16	12	5.22	**<0.0001**	***
***Synechococcus* (mg m^{-3})**					
High temp	16	12	7.045	**<0.0001**	***
High CO_2	16	12	-0.091	0.928	
High temp x high CO_2	16	12	10.739	**<0.0001**	***
Picophytoplankton (mg m^{-3})					
High temp	16	12	0.413	**0.679486**	
High CO_2	16	12	2.02	**0.043435**	*
High temp x high CO_2	16	12	3.773	**<0.0001**	***
Coccolithophores (mg C m^{-3})					
High temp	16	12	0.276	0.782	
High CO_2	16	12	-0.368	0.713	
High temp x high CO_2	16	12	-1.265	0.206	
Cryptophytes (mg C m^{-3})					
High temp	16	12	0.404	0.686	
High CO_2	16	12	0.273	0.785	
High temp x high CO_2	16	12	1.341	0.18	

Biogeosciences Discuss., https://doi.org/10.5194/bg-2017-510
Manuscript under review for journal Biogeosciences
Discussion started: 4 December 2017

Table 3. FRRf-based photosynthesis-irradiance curve parameters for the experimental treatments on the final day (T36).

Parameter	Control	sd	High temp	sd	High CO_2	sd	Combination	sd
P^B_m	2.77	1.63	9.58	1.94	18.93	2.65	3.02	0.97
α	0.03	0.01	0.09	0.01	0.13	0.01	0.04	0.00
I_k	85.33	45.47	110.93	6.09	144.13	17.91	86.38	33.06

Table 4. Results of generalised linear model testing for significant effects of temperature, CO_2 and temperature x CO_2 on phytoplankton photophysiology; P^B_m (maximum photosynthetic rates), α (light limited slope) and I_k (light saturated photosynthesis). Significant results are in bold; * p < 0.05, ** p < 0.001, *** p < 0.0001.

Response variable	n	*df*	*t*-value	*p*	sig
P^B_m					
High temp	12	8	7.353	**< 0.0001**	***
High pCO_2	12	8	8.735	**< 0.0001**	***
High temp x high pCO_2	12	8	-8.519	**< 0.0001**	***
α					
High temp	12	8	13.03	**< 0.0001**	***
High pCO_2	12	8	15.15	**< 0.0001**	***
High temp x high pCO_2	12	8	-14.82	**< 0.0001**	***
I_k					
High temp	12	8	2.018	0.0783	
High pCO_2	12	8	2.541	**0.0347**	*
High temp x high pCO_2	12	8	-2.441	**0.0405**	*